Singularities in a Modified Kuramoto-Sivashinsky Equation Describing Interface Motion for Phase Transition

Andrew J. Bernoff [a] and Andrea L. Bertozzi [b]

[a] *Dept. of Engineering Sciences & Applied Mathematics, Northwestern University, Evanston, IL 60208*

[b] *Dept. of Mathematics, University of Chicago, Chicago, IL 60637*

Abstract

Phase transitions can be modeled by the motion of an interface between two locally stable phases. A modified Kuramoto-Sivashinsky equation,

$$h_t + \nabla^2 h + \nabla^4 h = (1 - \lambda)|\nabla h|^2 \pm \lambda(\nabla^2 h)^2 + \delta\lambda(h_{xx}h_{yy} - h_{xy}^2),$$

describes near planar interfaces which are marginally long-wave unstable. We study the question of finite-time singularity formation in this equation in one and two space dimensions on a periodic domain. Such singularity formation does not occur in the Kuramoto-Sivashinsky equation ($\lambda = 0$). For all $1 \geq \lambda > 0$ we provide sufficient conditions on the initial data and size of the domain to guarantee a finite-time blow up in which a second derivative of h becomes unbounded. Using a bifurcation theory analysis, we show a parallel between the stability of steady periodic solutions and the question of finite-time blow up in one dimension. Finally, we consider the local structure of the blow up in the one-dimensional case via similarity solutions and numerical simulations that employ a dynamically adaptive self-similar grid. The simulations resolve the singularity to over 25 decades in $|h_{xx}|_{L^\infty}$ and indicate that the singularities are all locally described by a unique self-similar profile in h_{xx}. We discuss the relevance of these observations to the full intrinsic equations of motion and the associated physics.

1 Introduction

Problems of thermodynamic phase transition arise naturally in solidification, combustion and a host of other fields. If the transition region between two stable states is sufficiently narrow, the dynamics can often be approximated by an **interface motion** [25,51]. Examples include the solid/liquid interface in solidification [22,41,42], the combustion front separating burnt and unburnt combustants [25,45,51], and the motion of heteroclinic fronts connecting steady states in reaction-diffusion models [10,25,52].

One method of attack for these problems is to asymptotically reduce the partial differential equations governing the constituents in each phase to a simple equation of motion for the interface. If the system is isotropic, it is reasonable to expect that the normal velocity of the interface depends only on local geometrical properties, such as curvature (cf. Figure 1). In the early 1980's Langer [6,42] and Brower et al [15,16] introduced such an **intrinsic equation of motion** to model solidification. Their initially heuristic derivation prompted the study of formal asymptotic methods for the derivation of these equations.

The basic assumption that allows a reduction to interface dynamics is the smallness of the scale of variation of the constituents transverse to the interface (i.e. the boundary layer thickness) compared to the characteristic scale of variation along the interface. Denoting this ratio by ϵ, for small ϵ we obtain a perturbation expansion for the normal velocity of the interface, V,

$$V = \mu + \epsilon(\nu K) + \epsilon^2(\alpha K^2 + \beta Q) + \epsilon^3 \gamma \nabla_s^2 K + \mathcal{O}(\epsilon^3 K^3, \epsilon^4). \qquad (1)$$

Here K is the mean curvature, Q is the Gaussian curvature, ∇_s^2 is the surface Laplacian and $\mu, \nu, \alpha, \beta, \gamma$ are constants determined by the perturbation expansions. Note that at order ϵ^n the contribution to the velocity scales like $(length)^{-n}$ and that the terms appearing are isotropic descriptions of the local geometry of the surface.

Perhaps the first derivation of an equation of motion of this kind was the reduction of a one-component, symmetric, bistable reaction/diffusion model to an interface *motion by mean curvature* by Allen and Cahn heuristically [2] and more recently via matched asymptotics [52] and through the notion of a viscosity solution [18,24]. In this case only the curvature term in (1) has a non-zero coefficient and $\nu > 0$, in the $\epsilon \to 0$ limit. Note that $\nu > 0$ corresponds to curvature acting as a stabilizing influence; short-wave perturbations to the front are diffusively damped. The first two terms of this expansion, with $\nu > 0$, have been derived in the context of a one-component, bistable, reaction/diffusion systems; phase field models of combustion; and in models of excitable media [9,25,38,52,55]. In this case, a Burger's equation governs the

amplitude of near planar interfaces [33,58], and once again perturbations tend to be smoothed over long times.

When curvature is marginally destabilizing ($\nu < 0, |\nu| \ll 1$) it is possible to asymptotically balance this term with higher stabilizing terms in the expansion of the normal velocity. In particular, if $\gamma < 0$ short-wave perturbations to planar interfaces are damped. This observation motivated the derivation of this equation (1) by Sivashinsky & Frankel in the context of combustion [27–29]. The same equation was derived in the context of solidification of a hypercooled melt by Frankel [26,27], Umantsev & Davis [56], and Sarocka & Bernoff [53]. This equation can also arise for the motion of an interface in multicomponent bistable reaction/diffusion equations [10].

Frankel observed that for near planar solutions the intrinsic equation of motion reduces to the Kuramoto-Sivashinsky (KS) equation when the curvature term is marginally destabilizing. Here, we derive a more general amplitude equation by considering the near planar case when both μ and ν may be small. Following Sarocka & Bernoff, denote the location of the interface by $z = \tilde{h}(\tilde{x}, \tilde{y}, \tilde{t}) + \mu \tilde{t}$, where $|\nabla \tilde{h}| \ll 1$. In terms of this coordinate system V, K, Q and ∇_s^2 to leading order satisfy:

$$V \sim \tilde{h}_{\tilde{t}} - \frac{\mu}{2} |\nabla \tilde{h}|^2, \quad K \sim \frac{\nabla^2 \tilde{h}}{2}, \quad Q \sim \tilde{h}_{\tilde{x}\tilde{x}} \tilde{h}_{\tilde{y}\tilde{y}} - \tilde{h}_{\tilde{x}\tilde{y}}^2, \quad \nabla_s^2 \sim \nabla^2 \quad . \quad (2)$$

Here ∇ and ∇^2 denote derivatives with respect to the $(\tilde{x}, \tilde{y})$ coordinates. Rescaling the coordinates to balance leading order terms,

$$\tilde{t} = -\frac{2\gamma}{\nu^2} t, \qquad (\tilde{x}, \tilde{y}) = \epsilon \sqrt{\frac{\gamma}{\nu}} (x, y), \qquad \tilde{h} = \frac{\epsilon h}{\frac{\mu}{\nu} + \sigma \frac{\alpha}{2\gamma}}, \qquad (3)$$

yields

$$h_t + \nabla^2 h + \nabla^4 h = (1 - \lambda) |\nabla h|^2 + \sigma \lambda \left(\nabla^2 h \right)^2 + \delta \lambda \left(h_{xx} h_{yy} - h_{xy}^2 \right) \quad \text{(2D MKS)}$$

where

$$\sigma = \text{sgn}(\alpha \mu) = \pm 1,$$

$$\lambda = \frac{-\sigma \frac{\alpha}{2\gamma}}{\frac{\mu}{\nu} + \sigma \frac{\alpha}{2\gamma}}, \qquad 0 \leq \lambda \leq 1, \qquad (4)$$

$$\delta = -\sigma \frac{4\beta}{\alpha}, \qquad -\infty < \delta < \infty.$$

This paper addresses singularity formation in this two-dimensional modified Kuramoto-Sivashinsky equation (2D MKS). This rescaling is valid in the limit $|\nu| \to 0$; note that if $|\nu| \ll \mu$ that $\lambda \to 0$ recovers the standard KS equation.

3

The distinguished limit of both μ and ν tending to zero, with $\mu/\nu \sim \mathcal{O}(1)$, yields the terms proportional to $(\nabla^2 h)^2$ and $h_{xx}h_{yy} - h_{xy}^2$ in the near planar theory (2D MKS); these terms are generated from the K^2 and Q terms in the intrinsic equation of motion (1) respectively. As we show below it is the effect of the $(\nabla^2 h)^2$, not present in KS, that drives the finite-time blow up.

We also consider the one-dimensional version (1D MKS) of (4); if $h(x, y, t) = h(x, t)$ then we obtain

$$h_t + h_{xx} + h_{xxxx} = (1 - \lambda)h_x^2 + \sigma\lambda h_{xx}^2 \ . \qquad\qquad \text{(1D MKS)}$$

We present calculations of the 1D MKS on a periodic domain and show that the singularities all exhibit self-similar structure in h_{xx}.

The question of finite-time blow up has appeared briefly in the literature. Hocherman and Rosenau [35] discuss a large class of KS-type equations in one dimension and conjecture that a subclass with a suitable second-order nonlinearity, including the 1D MKS with $\lambda = 1$, yield a finite-time blow up. Hyman et al [36] discuss numerical simulations of a modification of the 1D MKS with $\lambda = 1$ and note that blow up does occur for certain initial data. However, their calculations seem to show only the early stages of the onset of the singularity and in particular do not discuss a similarity profile. Elliot and Zheng [23] prove blow up in the one-dimensional Cahn-Hilliard equation with a cubic nonlinearity. Their method would work for the 1D MKS with $\lambda = 1$ if the term h_{xx}^2 were replaced with h_{xx}^3. Furthermore, Novick-Cohen [48,49] discusses the blow-up problem for an equation corresponding here to the case $\delta = 0$, $\lambda = 1$ in both one and two dimensions. She shows that a blow up in the magnitude of a second derivative is necessary for singularity formation and presents one family of initial conditions in one dimension that guarantee blow up. Our analytical results slightly sharpen this necessary condition for blow up and extend the proof to the case where $\lambda \neq 1$ (necessitating the use of some ideas from the KS theory) and also to the case of nonzero δ. Furthermore, we consider the coupling of the first two Fourier modes in proving blow-up results and hence can draw parallels between bifurcation of steady solutions and the existence of finite-time blow up.

We briefly mention some related work on blow up in other nonlinear parabolic equations. A well known example is the second-order *semi-linear heat equation* for which the use of similarity variables provides much insight [30,31,57]. We mention that Budd et al [17] consider this equation with a conserved first integral and use the Fourier space method considered here to prove finite-time blow up. There has also been some recent work on singularity formation in degenerate fourth-order problems [11–13] in which the nonlinearity produces a 'second-type' [5] self-similar singularity in which the solution extinguishes at a point ($h \to 0$) and the blow up is in a higher derivative. We also point out the well known problem of self-similar blow up in the nonlinear Schrödinger

equation [43,44].

This paper is organized as follows: In Section 2 we present a proof that the solution to the MKS exists at least for a finite time and that if blow up occurs it is governed by a singularity in the second derivative of the amplitude. We then use, in Section 3, the Fourier method of Palais to provide sufficient conditions on the initial data to guarantee such a blow up. Section 4 discusses the relationship between the Palais blow-up proof and a bifurcation theory analysis of steady solutions. In Section 5 we demonstrate that a similarity solution exists describing self-similar finite-time blow up in the second derivative. In Section 6 we present numerical computations confirming this self-similar blow up scenario. We summarize our results in Section 7 and discuss their implications for the full intrinsic equations and the physical problems they model. In the appendix we describe the self-similar adaptive mesh scheme used to numerically study singularity formation in the 1D MKS.

2 Existence and Continuation of Solutions

In Section 3 we present sufficient conditions on the initial data to insure finite-time singularities in the 2D MKS,

$$h_t + \nabla^2 h + \nabla^4 h = (1 - \lambda)|\nabla h|^2 + \sigma\lambda \left(\nabla^2 h\right)^2 + \delta\lambda \left(h_{xx}h_{yy} - h_{xy}^2\right).$$

To prove these results we use the method of Palais which makes use of a comparison principle in Fourier space. In certain parameter ranges, the equation preserves the sign of the Fourier coefficients, hence blow up in a finite-dimensional subsystem is sufficient to prove blow up in the full PDE.

However, to correctly use this method we must first establish a continuation result for the equation. As pointed out in the eloquent paper by Ball [4] and also by Palais [50], a common error in using any comparison technique to prove blow up is to assume that the behavior of the comparison system is what actually drives the singularity. In fact the comparison principle holds only on a *time interval on which the solution exists*. For example, the singularity in the PDE might occur before the blow up in the subsystem and might not exhibit a singularity in the quantity which blows up for the subsystem. Indeed our numerical results in Section 6 demonstrate that this is the behavior for the 1D MKS since the Fourier modes remain bounded as the singularity forms. We caution all readers that a suitable continuation theorem is necessary before a valid proof of blow up can be established. To this end we prove the following theorem:

Theorem 1 *(Necessary condition for blow up) Consider the 2D MKS equa-*

tion with initial condition $h_0 \in H^{3+\epsilon}(S^2)$, $\epsilon > 0$. Then there exists a maximal interval of existence $[0, T^*)$ (with T^* possibly infinite) and a unique solution of the 2D MKS

$$h(x, y, t) \in C^\infty(0, T; C^\infty(S^2)) \cap C^1([0, T]; H^{3+\epsilon}(S^2)), \quad \forall T < T^*$$

with $h(x, y, 0) = h_0(x, y)$. Moreover if $T^* < \infty$, then necessarily $\int_0^t |D^2 h|^2_{L^\infty} dt \to \infty$ as $t \to T^*$.

Notation: in the above we use $|D^2 h|_{L^\infty}$ to denote the L^∞ norm of the Hessian matrix of the amplitude h.

Remarks: The theorem also holds for the 1D MKS as well; the proof can be made simpler. The ϵ in $H^{3+\epsilon}$ is necessary only for the proof in two dimensions and results from the fact that the Sobolev space H^m is a Banach algebra only for $m > n/2$.

Proof. We prove the theorem in two steps. First we appeal to an abstract theorem for semilinear parabolic equations to establish the local existence and uniqueness results and maximal interval of existence with a weaker blow-up condition. Then we prove the stronger blow-up condition via Sobolev space estimates and a standard Gronwall inequality.

We use the following abstract theorem for existence and continuation of a solution of a semilinear parabolic equation. The reader is referred to Ball [4] for more details:

Theorem 2 *(Ball [4]) Consider the equation*

$$\dot{u} = Au + f(u) \tag{5}$$

where A is the generator of a holomorphic semigroup $S(t)$ of bounded linear operators on a Banach space X. Suppose that $\|S(t)\| \leq M$ for some constant $M > 0$ and all $t \in \mathbb{R}^+$. Under these hypotheses the fractional powers $(-A)^{-\alpha}$ can be defined for $0 \leq \alpha < 1$ and $(-A)^\alpha$ is a closed linear operator with domain $X_\alpha = Domain((-A))^\alpha$ dense in X. Let $f(u)$ be locally Lipschitz, i.e. for each bounded subset U of X_α there exists a constant C_U so that

$$\|f(u) - f(v)\| \leq C_U \|u - v\|_\alpha \quad \forall u, v \in U.$$

Then given $u_0 \in X$, there exists a finite time interval $[0, t)$ and a unique solution to (5) with $u(\cdot, 0) = u_0$ on that time interval and the solution can be continued uniquely on a maximal interval of existence $[0, T^*)$. Moreover, if $T^* < \infty$ then necessarily

$$\lim_{t \to T^*} \|u(t)\|_\alpha = \infty.$$

We directly apply Theorem 2 to the 2D MKS with $\alpha = (3 + \epsilon)/4$, $A = -\nabla^4$, $X = L^2(S^1)$ and

$$f(u) = -\nabla^2 u + (1 - \lambda)|\nabla u|^2 + \sigma\lambda \left(\nabla^2 u\right)^2 + \delta\lambda \left(u_{xx}u_{yy} - u_{xy}^2\right).$$

Then $X_\alpha = H^{3+\epsilon}$ and

$$\|f(u) - f(v)\|_{L^2} \leq \|u - v\|_{H^2} + C(\lambda, \delta)(|D^2 u|_{L^\infty} + |D^2 v|_{L^\infty})\|u - v\|_{H^2}$$
$$+ (1 - \lambda)(|\nabla u|_{L^\infty} + |\nabla v|_{L^\infty})\|u - v\|_{H^1} \leq C(\|u\|_{H^{3+\epsilon}} + \|v\|_{H^{3+\epsilon}})(\|u - v\|_{H^2}).$$

Hence f is locally Lipschitz continuous on $H^{3+\epsilon}$. The direct application of the theorem implies that a solution exists on any time interval in which the $H^{3+\epsilon}$ norm is controlled.

We now finish the proof of Theorem 1 by showing that the $H^{3+\epsilon}$ norm is a priori controlled by $|D^2 h|_{L^\infty}$. (Recall that this denote the L^∞ norm of the Hessian matrix of h).

The proof uses some ideas from [47] for the Kuramoto-Sivashinksy equation.

We have

$$\frac{d}{dt}\frac{1}{2}\int h^2 = -\int |\nabla^2 h|^2 + \int |\nabla h|^2$$
$$+ (1 - \lambda)\int h|\nabla h|^2 + \lambda\sigma\int h|\nabla^2 h|^2 + \delta\lambda\int (h_{xx}h_{yy} - h_{xy}^2)h. \quad (6)$$

Note that

$$\frac{d}{dt}\frac{1}{2}\int |\nabla h|^2 = -\lambda\sigma\int (\nabla^2 h)^3 + \int |\nabla^2 h|^2 - \int |\nabla^3 h|^2$$
$$- 2(1 - \lambda)\int h_x^2 h_{yy} - \delta\lambda\int (h_{xx}h_{yy} - h_{xy}^2)\nabla^2 h \quad (7)$$

implies

$$\frac{d}{dt}\frac{1}{2}\int |\nabla h|^2 \leq C(\delta, \lambda)(|D^2 h|_{L^\infty} + 1)\int |\nabla^2 h|^2 - \tfrac{1}{2}|\nabla^3 h|^2. \quad (8)$$

Using

$$\int |\nabla^2 h|^2 \leq (\int |\nabla^3 h|^2)^{1/2}(\int |\nabla h|^2)^{1/2} \quad (9)$$

we have

$$\frac{d}{dt}\frac{1}{2}\int |\nabla h|^2 \leq C'(\delta, \lambda)(|D^2 h|_{L^\infty} + 1)^2\int |\nabla h|^2.$$

Gronwall's lemma then implies

$$\int |\nabla h(\cdot, t)|^2 \leq \int |\nabla h(\cdot, 0)|^2 e^{\int_0^t C'(\delta, \lambda)(|D^2 h|_{L^\infty} + 1)^2 dt}. \quad (10)$$

Furthermore, (8) and (9) imply that

$$\frac{1}{2}\int_0^T \int |\nabla^3 h|^2 \leq C'(\delta,\lambda)\int_0^T \left[(|D^2 h|_{L^\infty} + 1)(\int |\nabla^3 h|^2)^{1/2}(\int |\nabla h|^2)^{1/2}\right]$$

$$\leq C'(\delta,\lambda)\sup_{[0,T]}|\nabla h|_{L^2}\left[\int_0^T (|D^2 h|_{L^\infty} + 1)^2\right]^{1/2}\left[\int_0^T \int |\nabla^3 h|^2\right]^{1/2}$$

$$\int_0^T \int |\nabla^3 h|^2 \leq 4C'(\delta,\lambda)^2\left[\int_0^T (|D^2 h|_{L^\infty} + 1)^2\right]\int |\nabla h(\cdot,0)|^2 e^{\int_0^T C'(\delta,\lambda)(|D^2 h|_{L^\infty} + 1)^2 dt}. \tag{11}$$

Now note that
$$|\int |\nabla h|^2 h| \leq \|\nabla h\|_{L^2}\|\nabla h\|_{L^4}\|h\|_{L^4}.$$

Using the embedding of $W^{2,2}(S^2)$ in $W^{1,4}(S^2)$ [1] and interpolation in the Sobolev spaces we have

$$|\int |\nabla h|^2 h| \leq C\|\nabla h\|_{L^2}(\|h\|_{L^2}^2 + \|\nabla^2 h\|_{L^2}^2).$$

Equation (6) then implies

$$\frac{d}{dt}\int h^2 \leq -\int |\nabla^2 h|^2 + \int |\nabla h|^2$$

$$+ C(\delta)\lambda|D^2 h|_{L^\infty}^2(\int h^2)^{1/2} + (1-\lambda)C\|\nabla h\|_{L^2}(\|h\|_{L^2}^2 + \|\nabla^2 h\|_{L^2}^2).$$

A second application of Gronwall's lemma, using (10), shows that $\int h^2$ is a priori bounded on any time interval on which $\int_0^t |D^2 h(\cdot,s)|_{L^\infty}^2 ds$ is controlled.

Now estimate $\|\nabla^m h\|_{L^2}$ $m \geq 3$ using

$$\frac{d}{dt}\frac{1}{2}\int |\nabla^m h|^2 = -\int |\nabla^{m+2} h|^2 + \int |\nabla^{m+1} h|^2$$

$$+ \int \nabla^m\left(\sigma\lambda|\nabla^2 h|^2 + \delta\lambda(h_{xx}h_{yy} - h_{xy}^2)\right)\nabla^m h + (1-\lambda)\int \nabla^m|\nabla h|^2\nabla^m h.$$

This implies

$$\frac{d}{dt}\frac{1}{2}\int |\nabla^m h|^2 \leq -\int |\nabla^{m+2} h|^2 + \int |\nabla^{m+1} h|^2$$

$$+ C(\lambda,\delta)\|(D^2 h)^2\|_{H^m}(\int |\nabla^m h|^2)^{1/2} + (1-\lambda)\|(\nabla h)^2\|_{H^m}(\int |\nabla^m h|^2)^{1/2}. \tag{12}$$

We now apply the following calculus inequality in the Sobolev spaces [40]: *For all $m \in \mathbb{Z}^+ \cup \{0\}$, there exists $c > 0$ such that for all $u,v \in L^\infty \cap H^m(S^N)$*

$$\|uv\|_{H^m} \leq c\{|u|_{L^\infty}\|D^m v\|_{L^2} + \|D^m u\|_{L^2}|v|_{L^\infty}\}. \tag{13}$$

8

This gives

$$\frac{d}{dt}\frac{1}{2}\int |\nabla^m h|^2 \leq -\int |\nabla^{m+2} h|^2 + \int |\nabla^{m+1} h|^2$$
$$+ C(\delta)\lambda |D^2 h|_{L^\infty} (\int |\nabla^{m+2} h|^2)^{1/2}(\int |\nabla^m h|^2)^{1/2}$$
$$+ (1-\lambda)|\nabla h|_{L^\infty}(\int |\nabla^{m+1} h|^2)^{1/2}(\int |\nabla^m h|^2)^{1/2}. \quad (14)$$

Using

$$\int |\nabla^{m+1} h|^2 \leq \|\nabla^{m+2} h\|_{L^2}\|\nabla^m h\|_{L^2}$$

and maximizing over all $\|\nabla^{m+2} h\|_{L^2}$ gives

$$\frac{d}{dt}\frac{1}{2}\int |\nabla^m h|^2 \leq C(\delta)(1 + \lambda|D^2 h|_{L^\infty} + |\nabla h|_{L^\infty})^2 \int |\nabla^m h|^2.$$

Applying Gronwall's lemma gives

$$\int |\nabla^m h|^2(T) \leq \int |\nabla^m h|^2(0) e^{\int_0^T C(\delta)(1+\lambda|D^2 h(\cdot,s)|_{L^\infty}+|\nabla h|_{L^\infty})^2 ds}.$$

The fact that $|\nabla h|^2_{L^\infty} \leq C\int |\nabla^3 h|^2$ in 1 and 2-D and (11) implies that all higher Sobolev norms are a priori bounded provided that we have a bound for $\int_0^t |D^2 h(\cdot, s)|^2_{L^\infty} ds$.

Remark: Setting $\lambda = 0$ in the above and noting that in one dimension (7) produces a bound on $\int h_x^2$ depending only on T, one can directly reproduce the well known global existence result [20,21,32,37,46,47] for the one-dimensional Kuramoto-Sivashinsky equation.

3 Proof of Blow Up via Palais' Fourier Method

We can combine the theorem above with the Fourier space method of Palais [50] to prove that blow up occurs in both the 1D and 2D MKS equations. For simplicity we start with the one-dimensional problem for which we prove the following blow-up theorem:

Theorem 3 *(Blow up of solutions to 1D MKS) Let $h(x,t)$ be a solution to the 1D MKS,*
$$h_t + h_{xx} + h_{xxxx} = (1-\lambda)h_x^2 + \sigma\lambda h_{xx}^2 ,$$
with initial condition h_0 on a period of length $2\pi/k$. Let us assume

$$\lambda \in (0,1], \quad \sigma = \pm 1,$$

9

and

$$k^2 > k_c^2 = \begin{cases} \frac{1-\lambda}{\lambda} & for & \sigma = 1 \\ \frac{1-\lambda}{2\lambda} & for & \sigma = -1 \end{cases} \quad . \tag{15}$$

Then, (1) For $k \leq 1$, there exists initial data, h_0, of arbitrarily small H^3 norm which produces a solution that blows up in finite time. (2) For $k > 1$, there exists sufficiently large initial data that yield a solution which blows up in finite time. In either case the blow up necessarily has $\int_0^t |h_{xx}|_{L^\infty}^2 \, dt \to \infty$ as $t \to T^*$.

In Sections 5 and 6 we present a similarity solution and numerical computations that indicate that the blow up also has $|h|_{L^\infty} \to \infty$ as $t \to T^*$. We conjecture that this is true in general although no proof is known.

Proof. Following Palais [50] we consider even periodic solutions on interval of length $2\pi/k$ and expand $h(x,t)$ in a Fourier series

$$\begin{aligned} h(x,t) &= \sum_{n=-\infty}^{\infty} \hat{h}_n(t) e^{ink} \qquad \hat{h}_n = \hat{h}_{|n|} \\ &= \sum_{n=0}^{\infty} \hat{h}_n(t)(2 - \delta_{0n}) \cos(nkx). \end{aligned} \tag{16}$$

The Fourier transform of the 1D MKS is

$$(\hat{h}_n)_t = \alpha_n \hat{h}_n + \sum_{p+q=n} \beta_{pq} \hat{h}_p \hat{h}_q \qquad n = 0, 1, 2 \ldots, \tag{17}$$

where

$$\alpha_n = (nk)^2 - (nk)^4 \qquad \beta_{pq} = \begin{cases} 0, & pq = 0 \\ \lambda k^4 p^2 q^2 \left(\sigma - \frac{1-\lambda}{\lambda k^2 pq} \right), & pq \neq 0 \end{cases} . \tag{18}$$

There is some arbitrariness in the definition of the β_{pq} due to the fact that the terms with indices (p,q) and (q,p) have the same functional form; by specifying that $\beta_{pq} = \beta_{qp}$ the coefficient is determined uniquely. Note also that if either p or q is zero that β_{pq} vanishes which indicates that the constant term $(\hat{h}_0)$ decouples from the system; for the purpose of the analysis below we can restrict ourselves to $n \geq 1$.

The system (17) is called **cooperative** if $\beta_{pq} \geq 0$ for all p, q. Palais shows that the evolution of the $\hat{h}_n$ for any finite subsystem of (17) serves as a lower bound for the $\hat{h}_n$ of the full system provided that the full system is cooperative and

10

that the initial condition satisfies

$$\hat{h}_n(0) \geq 0 \quad \text{for all } n. \tag{19}$$

Note that if $\beta_{pq} \leq 0$ for all $p + q = n > 0$ that the system can be transformed into a cooperative system by letting $h(x,t) \rightarrow -h(x,t)$ and $\hat{h}_n \rightarrow -\hat{h}_n$. Since on any interval of existence of the full solution, the coefficients in the subsystem majorize the coefficients in the full system, a blow up in the subsystem means that the full system does not have a global solution. We reemphasize that this does not however signify a blow up of the Fourier coefficients in the full system because the singularity in the full system may occur well *before* the blow up in the subsystem.

To determine when the system (17) is cooperative, note that when $\sigma = 1$ and $pq \neq 0$ that $\beta_{pq}/(k^4 p^2 q^2)$ is minimized when $p = q = 1$ leading to the conclusion that $\beta_{pq} \geq 0$ for (15). Similarly, when $\sigma = -1$, note that $\beta_{pq}/(k^4 p^2 q^2)$ is maximized when $p = 1, q = -2$ (n. b. that for $p = 1, q = -1$ is disallowed as $n = p + q = 0$) leading to the conclusion that $\beta_{pq} \leq 0$ for (15). Hence, equation (17) has cooperative structure or can be transformed into a cooperative system when (15) is satisfied.

To finish the proof of blow up, consider the $n = 1$, $n = 2$ subsystem. As in Palais [50], given an initial condition satisfying (19) and k satisfying (15), on any time interval of existence the Fourier coefficients of the solution must be bounded from below by the solution of the 1-2 subsystem of (17),

$$(\hat{h}_1)_t = \alpha_1 \hat{h}_1 + 2\beta_{-12} \hat{h}_1 \hat{h}_2$$

$$(\hat{h}_2)_t = \alpha_2 \hat{h}_2 + \beta_{11} \hat{h}_1^2. \tag{20}$$

Following Lemma 4.5 in [50] we see that if $k \leq 1$ then $\alpha_1 > 0$ and arbitrarily small initial amplitudes give finite-time blow up. For $k > 1$ Lemma 4.5 of [50] requires $\alpha_1 > \alpha_2$ (which is always true) to show that sufficiently large initial conditions blow up. Note that when $k = k_c$ either β_{11} or β_{-12} vanishes, and although the system (17) remains cooperative, the 1-2 subsystem does not exhibit finite-time blow up. For this case an exact solution exists for both the full problem and the 1-2 subsystem which blows up only in infinite time (cf. Sarocka & Bernoff [53]).

Thus the solution can not be continued forever and must have a finite-time singularity. From Theorem 1 this implies that $\int_0^t |h_{xx}|_{L^\infty}^2 dt$ becomes unbounded.

Section 4 provides a more graphical exposition of this result indicating the regions of k where small and finite amplitude blow up occur and relating these results to the bifurcation of a branch of periodic solutions at $k = 1$.

11

The limit $\lambda \to 0$ recovers the Kuramoto-Sivashinsky equation which does not exhibit blow up in one dimension. In this limit both k_c and the amplitude of the perturbation needed to ensure blow up from Theorem 3 both tend to infinity. We believe that for sufficiently small λ that some finite amplitude initial conditions will lead to bounded dynamics which qualitatively resemble what is seen for the Kuramoto-Sivashinsky equation while some set of large amplitude initial conditions will lead to finite-time blow up.

Note that the one-dimesional blow-up results provides a set of initial conditions, in which the profile is independent of one of the space variables, that yield blow up in two dimensions as well. In fact, one can apply Palais' method to obtain a much larger set of initial conditions that also yield blow up in the 2D MKS. We state such a theorem below.

Theorem 4 *(Blow up of solutions to 2D MKS) Let $h(x, y, t)$ be a solution to 2D MKS,*

$$h_t + \nabla^2 h + \nabla^4 h = (1 - \lambda)|\nabla h|^2 + \sigma\lambda \left(\nabla^2 h\right)^2 + \delta\lambda \left(h_{xx}h_{yy} - h_{xy}^2\right),$$

with initial condition h_0 on a periodic rectangle with sides $(2\pi/k_1, 2\pi/k_2)$. Assume

$$\lambda \in (0, 1], \quad \sigma = \pm 1,$$

$$k_1^2, k_2^2 > k_c^2, \tag{21}$$

and

$$\begin{aligned} \delta \geq -1 \quad &for \quad \sigma = 1 \\ \delta \leq 1 \quad &for \quad \sigma = -1 \end{aligned}. \tag{22}$$

Then, (1) If k_1 or $k_2 \leq 1$, there exists initial data of arbitrarily small H^4 norm which produces a solution that blows up in finite time. (2) For k_1 and $k_2 > 1$, there exists sufficiently large initial data that yield a solution which blows up in finite time. In either case the blow up necessarily has $\int_0^t |D^2 h|_{L^\infty}^2 dt \to \infty$ as $t \to T^*$.

Remarks: Recall from Section 1 that $|D^2 h|_{L^\infty}$ denotes the L^∞ norm of the Hessian of h. Additional ranges of the parameters can also be studied using this method. For ease of exposition we present a proof that addresses (22).

Proof. Consider even, doubly periodic solutions on a rectangle with sides $(2\pi/k_1, 2\pi/k_2)$. Consequently $h(x, y, t)$ can be written as a double Fourier series,

$$h(x, y, t) = \sum_{n=-\infty}^{\infty} \sum_{m=-\infty}^{\infty} \hat{h}_{nm}(t) e^{i(nk_1 x + mk_2 y)} \qquad \hat{h}_{nm} = \hat{h}_{|n||m|}$$

$$= \sum_{n=0}^{\infty} \sum_{m=0}^{\infty} \hat{h}_{nm}(t)(2 - \delta_{0n})(2 - \delta_{0m}) \cos(nk_1 x) \cos(mk_2 y). \qquad (23)$$

Substituting this Fourier series into (4) yields

$$(\hat{h}_{nm})_t = \alpha_{nm} \hat{h}_{nm} + \sum_{p+r=n} \sum_{q+s=m} \gamma_{pqrs} \hat{h}_{pq} \hat{h}_{rs} \qquad n, m = 0, 1, 2 \ldots \qquad (24)$$

where

$$\alpha_{nm} = (nk_1 + mk_2)^2 - (nk_1 + mk_2)^4$$

$$\gamma_{pqrs} = \beta_{pr}(k_1) + \beta_{qs}(k_2) + \lambda k_1^2 k_2^2 \left[\sigma(p^2 s^2 + q^2 r^2) + \frac{\delta}{2}(ps - qr)^2 \right]$$

$$= \beta_{pr}(k_1) + \beta_{qs}(k_2) + \lambda k_1^2 k_2^2 \left[(\sigma + \delta)(p^2 s^2 + q^2 r^2) - \frac{\delta}{2}(ps + qr)^2 \right].$$

Here $\beta_{pr}(k_1)$ is just β_{pr} evaluated at k_1 instead of k. Once again we have chosen $\gamma_{pqrs} = \gamma_{rspq}$ to eliminate any arbitrariness in the expansion. Note that if either p and q or r and s are zero that γ_{pqrs} vanishes, which indicates that the constant term ($\hat{h}_{00}$) decouples from the system; for the purpose of the analysis below we can restrict ourselves to n, m nonnegative and not both zero.

The system (24) is cooperative when $\gamma_{pqrs} \geq 0$ (for $\sigma = 1$) or $\gamma_{pqrs} \leq 0$ (for $\sigma = -1$). The constraint (21) arises in an exactly parallel fashion as (15) when considering $\beta_{pr}(k_1)$ (corresponding to $q = s = 0$) and $\beta_{qs}(k_2)$ (corresponding to $p = r = 0$). The second constraint (22) is sufficient to assure that the remaining term in γ_{pqrs} has the appropriate sign.

Hence, equation (24) has cooperative structure or can be transformed into a cooperative system when (21,22) are satisfied. Note that the subsystems generated by ($\hat{h}_{10}, \hat{h}_{20}$) and ($\hat{h}_{01}, \hat{h}_{02}$) have the exact same structure as the 1-2 subsystem (20) with k replaced by k_1 and k_2 respectively. Consequently, consideration of these subsystems again leads to the conclusions of the theorem.

Remark: While the theorems presented here give sufficient conditions for blow up, our numerical results show that blow up can occur for a much larger class of initial conditions. In Section 5 and 6 we show that the blow up in 1D MKS is actually characterized by a similarity solution in h_{xx}. The similarity solution does not exhibit a blow up in the L^2 norm of h but in the L^∞ norm and in higher Sobolev norms. This lack of blow up in the L^2 norm indicates that in the limit as $t \to t_c$, all of the Fourier modes remain bounded but that the decay of h_n is bad as $n \to \infty$. We conjecture that any initial condition

13

with h_{xx} locally close enough to the similarity profile will exhibit a finite-time blow up.

4 Bifurcation Theory and its Relationship to the Blow-up Results

This section addresses the relationship between the bifurcation of periodic solutions from a uniform planar state to the blow-up results proved in the previous section. We consider the 1D MKS:

$$h_t + h_{xx} + h_{xxxx} = (1 - \lambda)h_x^2 + \sigma\lambda h_{xx}^2 \ . \qquad \text{(1D MKS)}$$

A cursory examination of the problem suggest that bifurcation from the planar state should be unrelated to finite-time blow up since the blow-up proof deals with a fully nonlinear phenomena (blow up) and the bifurcation theory deals with the weakly nonlinear regime. However, since the 1D MKS possesses a purely quadratic nonlinearity, both the proof of blow up and the bifurcation analysis reduce to a study of the 1-2 subsystem of Fourier modes. Below we review the bifurcation theory for periodic states in the system, present numerical continuation of the bifurcation branches, and relate these results to Theorem 3 on blow up discussed in the previous section.

4.1 Bifurcation analysis of periodic solutions

Sarocka and Bernoff [53] discuss the bifurcation of the planar state to periodic solutions for the 1D MKS with $\sigma = 1$; we review these results and extend them to the case $\sigma = -1$. We use center manifold theory [34] as this elucidates the connection with the 1-2 subsystem discussed in the context of the Palais theory. The Fourier transform of the 1D MKS converts the PDE into a countably infinite coupled system of ODE's (17). The $n = 0$ mode is the average of h on the interval. This mode is driven by the other modes but does not appear in the equations for the remaining modes, reflecting the translational invariance of the underlying physical problem.

The *linear* growth rate of $\hat{h}_n$ (about the zero state) is $\alpha_n = (nk)^2 - (nk)^4$. If we think of k as the bifurcation parameter (equivalent to changing the length of the interval) $\hat{h}_1$ undergoes a change in stability at $k = 1$. Consequently, at $k = 1$ the system possesses a one-dimensional center subspace ($\hat{h}_1$) with all the remainder modes lying in the stable subspace. A standard perturbation analysis of the center manifold then reveals the topology of the system of ODE's in a neighborhood of $k = 1$.

Proceeding with this *center manifold reduction*, we use the amplitude of the

1-mode, $\hat{h}_1$, as the expansion parameter and see that at order $(\hat{h}_1)^2$ only the $\hat{h}_0$ and $\hat{h}_2$ play a role. Recalling that the $n = 0$ mode decouples from the problem, the center manifold at order $\hat{h}_1^2$ can be approximated by:

$$\hat{h}_2 = -\frac{\beta_{11}}{\alpha_2}(\hat{h}_1)^2. \tag{25}$$

Substituting this expression into the amplitude equation for $\hat{h}_1$ gives the equation governing the evolution of $\hat{h}_1$ on the center manifold correct to order $(\hat{h}_1)^5$,

$$\begin{aligned}
(\hat{h}_1)_t &= \alpha_1 \hat{h}_1 - 2\frac{\beta_{11}\beta_{-12}}{\alpha_2}(\hat{h}_1)^3 \\
&= (k^2 - k^4)\hat{h}_1 - \frac{1}{3}(1 - \lambda - \sigma\lambda)(1 - \lambda + 2\sigma\lambda)(\hat{h}_1)^3 \tag{26}
\end{aligned}$$

which is valid near the bifurcation point $k = 1$; note that the coefficient of the cubic term is evaluate at $k = 1$.

Equation (26) describes a pitchfork bifurcation from the planar state to a periodic solution. When the coefficient of the cubic term is negative (positive) the bifurcation is supercritical (subcritical) to a stable (unstable) state specified by

$$\begin{aligned}
(\hat{h}_1)^2 &= \frac{\alpha_1\alpha_2}{2\beta_{11}\beta_{-12}} + \mathcal{O}\left((k-1)^2\right) \\
&= \frac{72(k-1)}{(1 - \lambda - \sigma\lambda)(1 - \lambda + 2\sigma\lambda)} + \mathcal{O}\left((k-1)^2\right). \tag{27}
\end{aligned}$$

Hence, there is a transition from a supercritical to a subcritical bifurcation at $\lambda = \lambda_c$ where $\lambda_c = 1/2$ for $\sigma = 1$ (Figure 2a) and $\lambda_c = 1/3$ for $\sigma = -1$ (Figure 2b). For $\lambda < \lambda_c$ the branch of solutions is stable, at least to perturbations with the same period, whereas for $\lambda > \lambda_c$ the initial bifurcation is to an unstable state. Below we extend these curves numerically to the fully nonlinear regime. There are two branches that bifurcate from $k = 1$, corresponding to positive and negative values of $\hat{h}_1$; in fact these branches are the same solution spatially translated by half a period (cf. [3,39]).

4.2 Numerical extension of periodic solutions

To compute these branches of one-dimensional periodic solutions for the 1D MKS we integrate the steady state equation,

$$h_{xxxx} + h_{xx} = \sigma\lambda h_{xx}^2 + (1 - \lambda)h_x^2, \tag{28}$$

numerically with a shooting method as was done in Sarocka & Bernoff [53].

15

The results are presented in Figures 2a,b. The branch corresponding to the standard KS equation ($\lambda = 0$) agrees with the primary bifurcation branch found by Kevrekidis, Nicolaenko, and Scovell [39] in their numerical study of the KS equation and terminates in a secondary bifurcation to a solution with half the spatial period. As λ increases the bifurcation branch becomes vertical at λ_c where the bifurcation goes from supercritical to subcritical. For $\lambda = 1/2$ and $\sigma = 1$ the exact solution $h(x,t) = \frac{1}{2}G_0^2 t + F_0 + G_0 \cos x$ yields a perfectly vertical bifurcation [53]. The subcritical branches appear to asymptote to a constant amplitude for increasing wavenumber (outside the range of these figures).

4.3 The relationship between the Palais blow-up results & bifurcation theory

There is an interesting parallel between the blow-up Theorem 3 and the bifurcation theory discussed above: *both sets of results are governed by the 1-2 subsystem of Fourier modes.* Recall from section 3 that the cooperativity of 1-2 subsystem

$$(\hat{h}_1)_t = \alpha_1 \hat{h}_1 + 2\beta_{-12}\hat{h}_1\hat{h}_2$$

$$(\hat{h}_2)_t = \alpha_2 \hat{h}_2 + \beta_{11}\hat{h}_1^2 \tag{29}$$

implies the cooperativity of the full system and that the set of initial conditions that lead to blow up in (29) determine a class of initial conditions that lead to blow up in the full system. Note also that the 1-2 subsystem reproduces the perturbation expansion from the bifurcation theory analysis to order $\hat{h}_1^5$. Consequently, the branches of solutions originating in the pitchfork bifurcation at $k = 1$ in the 1-2 subsystem is tangent to the branch of solutions for the full system. Below, we first show the behavior of the 1-2 subsystem divides into two cases depending on whether the pitchfork bifurcation is sub- or supercritical. We then analyze the behavior of the system in each case.

The proof of blow up from the previous section relies on a comparison principle in Fourier space; the system (17) is cooperative when the coefficients, β_{pq}, of all the nonlinearities have the same sign. In particular, the system is cooperative when the product $\beta_{11}\beta_{-12}$ is positive. This determines a critical value of k, $k = k_c$ (as a function of λ and σ) such that when $k > k_c$ the system is cooperative. Moreover, this condition at $k = 1$ is exactly what distinguishes a subcritical from a supercritical bifurcation; when $k_c > 1$ the bifurcation is supercritical and when $k_c < 1$ the bifurcation is subcritical. The bifurcation is vertical for the critical value of λ such that $\lambda = \lambda_c$ such that $k_c = 1$. Table 1 summarizes these critical values:

Table 1: Critical values of λ and k

	$\sigma = 1$	$\sigma = -1$
Cooperativity ($k > k_c$)	$k_c = \sqrt{\frac{1-\lambda}{\lambda}}$	$k_c = \sqrt{\frac{1-\lambda}{2\lambda}}$
Bifurcation Structure ($k_c(\lambda_c) = 1$)	$\lambda_c = 1/2$	$\lambda_c = 1/3$

The dynamics of the system can now be separated into two cases; the supercritical case ($0 \leq \lambda < \lambda_c$) and the subcritical case ($\lambda_c < \lambda \leq 1$). The features of each are described in table 2:

Table 2: Dynamical features of 1-2 subsystem

Supercritical vs. Subcritical cases

Bifurcation type	Supercritical	Subcritical
Range of λ	$0 \leq \lambda < \lambda_c$	$\lambda_c < \lambda \leq 1$
Location of k_c	$k_c > 1$	$k_c < 1$
Blow up from infinitesimal amplitude initial data	Absent	$k_c < k \leq 1$
Blow up from finite amplitude initial data	$k > k_c$	$k > 1$

Figures 3a,b illustrate the supercritical and subcritical cases respectively.

In the supercritical case (Figure 3a), the pitchfork bifurcation at $k = 1$ produces a stable branch of periodic solutions for k slightly below 1, while for $k > 1$ the zero solution is stable. For $k > k_c > 1$ the system is cooperative but requires sufficient large initial data satisfying (19) to produce a finite-time blow up. At $k = k_c$ in the 1-2 subsystem an unstable branch of steady solutions bifurcates from infinity. The Palais theory tells us that finite amplitude initial conditions will lead to finite-time blow up provided that $\hat{h}_1$ and $\hat{h}_2$ are in excess of the values along this branch and $\hat{h}_n$ is non-negative for $n \geq 1$. Note also that as λ tends to zero, corresponding to the well-posed Kuramoto-Sivashinsky limit, that k_c tends to infinity suggesting that blow up only occurs in the corresponding short-wave limit.

In the subcritical case (Figure 3b), the pitchfork bifurcation at $k = 1$ produces a branch of unstable periodic solutions for $k > 1$. Here $k_c < 1$. The Palais theory tells us that for $k_c < k < 1$ non-zero initial conditions will lead to finite-time blow up provided that $\hat{h}_n$ is non-negative for $n \geq 1$. In addition, the theory tells us that for $k > 1$ finite amplitude initial conditions will lead to blow up provided that $\hat{h}_1$ and $\hat{h}_2$ are in excess of the values along the unstable branch produced in the pitchfork bifurcation and $\hat{h}_n$ is non-negative

for $n \geq 1$. Note that in this region ($k > 1$) the zero solution is stable and locally attracting.

Taken together these observations suggest the following picture of the dynamics; for some values of k and λ almost all initial conditions lead to finite-time blow up. For other values, small initial conditions are attracted to either zero or periodic solutions, while some large amplitude perturbations lead to blow up. Some invariant set must separate the basins of attraction of these two behaviors. For the subcritical case the obvious candidate is the unstable branch of periodic solutions which bifurcates from $k = 1$ and its stable manifold. For the supercritical case, the situation is less clear; the well-studied chaotic dynamics for the Kuramoto-Sivashinsky problem [3,39,46] suggest that the phase space is much less orderly in this case.

5   Similarity Solution for the 1D MKS

This section describes properties of a similarity solution for the blow-up profile of the 1D MKS:

$$h_t + h_{xx} + h_{xxxx} = (1 - \lambda)h_x^2 + \sigma\lambda h_{xx}^2 . \qquad \text{(1D MKS)}$$

The self–similarity occurs in the second derivative h_{xx} (the curvature in the long wave theory), with a simple 'first-type' [5] scaling, in which the power laws in the blow up of the magnitude of h_{xx} and its characteristic length scale can be determined by dimensional analysis. This section describes analytical behavior of the similarity solution. We do not attempt here to prove that this self-similarity is the typical asymptotic behavior of a finite-time singularity. However the extremely well resolved numerical simulations of the full PDE, described in Section 6, suggest this to be a universal form for the blow-up profile. As we show below, two interesting features of the similarity solution are that (1) it is symmetric about the blow-up point and (2) there are *no free parameters* for either the time dependence or profile of the similarity solution. We conjecture that this is responsible for the universal blow-up behavior observed in the numerical simulations. Indeed even singularity formation resulting from *non-symmetric* initial data still exhibits this locally *symmetric* blow-up profile.

We conjecture that this self-similar route to blow up is **universal** over a large class of parameters and initial conditions for both the second derivative in the 1D MKS and the amplitude, h, in related equations such as the Sivashinsky equation that arises in directional solidification [22,48,49,54],

$$h_t + \alpha_0 h + h_{xx} + h_{xxxx} + (h^2)_{xx} = 0, \qquad (30)$$

Cahn-Hilliard type problems with quadratic potentials [23,49],

$$h_t + (h^2 \pm h + h_{xx})_{xx} = 0. \tag{31}$$

and the Childress-Speigel equation [19] which is equivalent to equation (31) after rescaling.

This section is organized as follows. First we propose similarity variables (in both time and space) and rescale the equation. A self-similar blow-up profile for h_{xx} then corresponds to a steady solution of a rescaled equation. We discuss several integrals associated with the similarity equation and in particular rewrite the rescaled evolution equation as a conservation law to reduce the steady fourth-order ODE to a third-order equation. The constant of integration provides a link between the behavior of the solution at the origin and the decaying behavior in the far-field. A WKB analysis of the far-field behavior is instrumental in studying the ODE as a boundary value problem on the half-line with an appropriate number of boundary conditions. We numerically compute a locally (and perhaps globally) unique solution of the ODE via a shooting method. Finally, we discuss the behavior of the solution in the original variables for both h and h_{xx}.

5.1 Similarity variables

Recall that the blow-up Theorem 3 states that the second derivative h_{xx} should develop a singularity. As the zero mode of h does not affect small scale structure of the solution, we look for a similarity solution to the evolution equation for $h_{xx} = p$.

Rewriting the 1D MKS in terms of p yields

$$p_t + p_{xx} + p_{xxxx} - \sigma\lambda(p^2)_{xx} - (1-\lambda)(h_x^2)_{xx} = 0. \tag{32}$$

If the singularity occurs for short length scales and large amplitudes, then $\sigma\lambda(p^2)_{xx}$ should dominate both $(1-\lambda)h_x^2$ and p_{xx}. We now balance the remaining three terms to uniquely determine appropriate time and space scales for the problem. First define a new variable

$$q(x,t) = \lambda p(x,t)/\sigma.$$

Equation (32) then becomes

$$q_t + q_{xxxx} - (q^2)_{xx} = \frac{\sigma(1-\lambda)}{\lambda}\left((\partial_x^{-1}q)^2\right)_{xx} - q_{xx} \approx 0. \tag{33}$$

The right hand side of (33) contains all the lower order terms that do not contribute to the similarity solution described below. We propose the similarity

solution as an *asymptotic* behavior locally near the singular point. Hence we look for a solution to the homogeneous equation

$$q_t + q_{xxxx} - (q^2)_{xx} = 0 \tag{34}$$

on the line $-\infty < x < \infty$.

The $\lambda \to 0$ limit in the 1D MKS yields the Kuramoto-Sivashinsky equation for which singularities are not possible. Note that in this limit the first term on the right hand side of (33) blows up. As shown in Section 4, it is this term that is simultaneously responsible for the transition from subcritical to supercritical bifurcation at the critical wavenumber $k = 1$ and for the need to take sufficiently large initial data to obtain finite-time blow up when λ is small. We see this latter effect in the search for a stable similarity solution in that in order for the RHS of (33) to be lower order, the solution must be large enough for the LHS to dominate the large coefficient in front of the $((\partial_x^{-1}q)^2)_{xx}$.

We consider a self-similar blow-up solution of the form

$$q(x,t) = \frac{f(x/A^r(t))}{A(t)}. \tag{35}$$

Substituting this into (34) and separating variables yields $A(t) = (t_c - t)^{1/2}$, $r = 1/2$. Rewriting (34) in terms of the similarity variables

$$s = -\ln(t_c - t) \qquad \eta = \frac{x - x_c}{(t_c - t)^{1/4}} \qquad f(\eta, s) = q(x,t)(t_c - t)^{1/2} \tag{36}$$

gives the following rescaled fourth-order PDE for f,

$$f_s + \tfrac{1}{2}(f + \frac{\eta f_\eta}{2}) = (f^2)_{\eta\eta} - f_{\eta\eta\eta\eta} \qquad -\infty < \eta < \infty, \tag{37}$$

which we refer to as the **similarity PDE**. A steady solution $(f(\eta, s) = F(\eta))$ produces a self-similar blow up profile for the original evolution equation for q. Plugging the scaling form (35) into the original equation (33) shows that right hand side terms scale as $(t_c - t)^{-1}$, a lower order behavior than $(t_c - t)^{-3/2}$ for the terms on the left hand side.

As is typical of such rescaled equations, the similarity PDE retains reflection symmetry about the origin $(\eta \to -\eta)$, but does not possess the the translation invariance in the spatial variable of the original equation due to the fact that we have used a time dependent dilation of space for the rescaling. However, the various translation symmetries in the original equation transform into more complicated invariances in the rescaled problem. The subject of these symmetries and there relationship to the stability of the similarity solution is beyond the scope of this paper. It would be interesting to know if some of the similarity variable techniques used to study problems like the semilinear

20

heat equation [5,30,31,57] might apply to such higher order nonlinear diffusion equations as well.

Some information about solutions to the similarity PDE can be obtained by considering the properties of the unscaled equation (33). In particular, as this equation takes the form of a conservation law,

$$q_t = \partial_x \left((q^2)_x - q_{xxx} \right),\tag{38}$$

the similarity PDE takes a related form,

$$\left(\partial_s + \partial_\eta \frac{\eta}{4} \right) f e^{s/4} = e^{s/4} \partial_\eta \left((f^2)_\eta - f_{\eta\eta\eta} \right),\tag{39}$$

where the differential operator on the left hand side computes the time rate of change with respect to the new time s of a quantity including a contribution from the dilating coordinate η.

Integrating this conservation law over the entire line tells us that the total area of q,

$$I_0 = \int_{-\infty}^{\infty} q \ dx,\tag{40}$$

which is conserved, is related to the total area of f by

$$\int_{-\infty}^{\infty} f \ d\eta = e^{-s/4} I_0.\tag{41}$$

Conservation of the integral of q implies that any steady solution F of the similarity PDE must have zero area and therefore obtain both positive and negative values (cf. Figure 4).

Since equation (34) is an evolution equation for the second derivative of a potential, the evolution of the first moment, $(x - x_c)q$ can also be written as a conservation law,

$$((x - x_c)q)_t = \partial_x \left((x - x_c)(q^2)_x - q^2 - (x - x_c)q_{xxxx} + q_{xxx} \right).\tag{42}$$

The related form for the similarity equation (37) is

$$\left(\partial_s + \partial_\eta \frac{\eta}{4} \right) \eta f = \partial_\eta \left(\eta(f^2)_\eta - f^2 - \eta f_{\eta\eta\eta} + f_{\eta\eta} \right).\tag{43}$$

The definition of the similarity variables (36) implies that the first moments of both q and f are equal and conserved,

$$I_1 = \int_{-\infty}^{\infty} (x - x_c)q \ dx = \int_{-\infty}^{\infty} \eta f \ d\eta.\tag{44}$$

21

Note that symmetric solutions have vanishing first moment but that solutions that decay like η^{-2} in the far field, as in the case of our similarity solution, have divergent integrands in (44).

5.2 Steady solutions to the similarity PDE

We now look for steady solutions of the similarity PDE to obtain similarity solutions describing the asymptotic behavior of blow up.

We integrate once the time independent version of the conservation form (43) to yield the following third-order ODE for the similarity profile,

$$\frac{\eta^2}{4}F + F^2 - \eta(F^2)_\eta + \eta F_{\eta\eta\eta} - F_{\eta\eta} = C. \tag{45}$$

Evaluating (45) at $\eta = 0$ produces a relationship between the integration constant C and the boundary values at $\eta = 0$,

$$C = F^2(0) - F_{\eta\eta}(0). \tag{46}$$

We can match the similarity profile to the integral order behavior away from the singular point by finding a far-field solution invariant under the similarity rescaling (36). This leads us to look for a solution F of (45) that decay like η^{-2} as $|\eta| \to \infty$. Examination of (45) shows that this decay must have a leading order behavior of $4C/\eta^2$.

To understand this behavior of (45) at infinity, we linearize this equation and apply a WKB analysis. The linear equation

$$\eta F_{\eta\eta\eta} - F_{\eta\eta} + \frac{\eta^2}{4}F = C \tag{47}$$

has a particular solution and three homogeneous solutions. For large $|\eta|$ the particular solution, F_P, has a regular Laurent expansion in inverse powers of η^{2+4n}

$$F_P(\eta) = \frac{4C}{\eta^2} + \sum_{n=1}^{\infty} \frac{c_n}{\eta^{2+4n}}. \tag{48}$$

WKB methods [1] applied to the homogeneous solutions $F_n, n = 0, 1, 2$ yield

---

[1] Alternatively, the homogeneous solution can be transformed into a hyper-Airy equation by the change of variables $G = F_{\eta\eta}/\eta$ and an integral representation can be found by a generalized Fourier transformation leading to a complete asymptotic expansion for F.

the asymptotic behavior for large η [7],

$$F_n(\eta) \sim |\eta|^{2/3} e^{-3\omega_n |\eta|^{4/3} 2^{-8/3}} \qquad \omega_n = \exp(n\frac{2\pi i}{3}) \ . \qquad (49)$$

Note that F_1 and F_2 grow exponentially; consequently, for the solution to remain bounded we specify that that

$$F(\eta) = F_P + b_1^{\pm} F_0 \qquad \text{as} \qquad \eta \to \pm\infty, \qquad (50)$$

corresponding to two boundary conditions at $\eta = \pm\infty$. We note that the nonlinear term introduces a $1/\eta^4$ correction to F_P and higher-order corrections to the asymptotic expansion of F_0, which may be safely ignored.

At first glance the problem seems over-specified, with four conditions (two each at $\pm\infty$) on a third-order equation. However, we have neglected to consider the reflection symmetry. Two possibilities exist for the solution; a symmetric solution invariant under $(\eta \to -\eta)$ or a non-symmetric pair of solutions mapped into each other by $(\eta \to -\eta)$. The non-symmetric case is indeed over specified, and we consider it unlikely that such a solution exists. However, the symmetric case yields only a single boundary condition at the origin,

$$F_\eta(0) = 0, \qquad (51)$$

yielding a total of three boundary conditions on a third-order ODE. Note that the values of F and its second derivative at the origin determine C through (46).

Recapitulating, this suggests the existence of a locally (perhaps globally) unique steady solution to the third-order ODE (45) that is symmetric about the origin, and decays in the far-field as $4C/\eta^2$. We numerically compute such a solution using a shooting method to yield the profile in Figure 4. In the next section we show that this solution has exceedingly good agreement with the blow-up profiles observed in our numerical solutions of the full 1D MKS equation.

The shooting method uses an iterative procedure to search for the special values of $F(0)$ and $F_{\eta\eta}(0)$. We integrate the non-linear ODE until its norm grew above a threshold, then linearize the equation and integrate a fixed distance further and project the solution onto the growing modes F_1 and F_2. An underrelaxed Newton-Rapheson method eliminates the growing modes in the far-field. Since this method converges only locally in parameter space, the initial guess for $F(0)$ and $F_{\eta\eta}(0)$ come from the numerical simulations of blow up in the 1D MKS. The far-field behavior of the ODE shows extreme sensitive dependence on initial conditions; the values of the initial condition need to be specified to a tolerance of 10^{-9} to suppress the growing modes at $\eta = 20$.

23

Numerically, we find that

$$F(0) = -2.168965546 \qquad F_{\eta\eta}(0) = 2.694018654 \tag{52}$$

which implies that the constant of integration in (45) is

$$C = \bar{C} \equiv 2.010392886. \tag{53}$$

Figure 4 graphs a profile of the steady solution.

The numerical evidence for the existence of this solution is convincing, coming from both the numerical solution of the 1D MKS and the steady solution to the similarity equation found with the shooting method. Indeed all our observations of a finite-time singularity exhibit precisely this asymptotic behavior. However, a proof of the the existence and in particular the uniqueness of this solution remains an open question.

5.3 *Behavior of the interface near singularity*

We now discuss the expected behavior of the profiles for h and h_{xx} if the above similarity solution describes the asymptotic blow-up behavior.

In the far-field, the steady similarity solution takes the form

$$F(\eta) \sim \frac{4\bar{C}}{\eta^2} + \frac{160\bar{C}(3 - 2\bar{C})}{\eta^6} \qquad \text{for} \qquad |\eta| \gg 1. \tag{54}$$

Transforming to the original (x, t) variables gives

$$q(x, t) \sim \frac{4\bar{C}}{(x - x_c)^2} + 160\bar{C}(3 - 2\bar{C})\frac{t_c - t}{(x - x_c)^6}$$
$$\text{for} \quad (t_c - t)^{1/4} \ll |x - x_c| \ll 1. \tag{55}$$

Note that $q(x, t)$ converges pointwise to the function $4\bar{C}/(x - x_c)^2$ in a neighborhood of the singularity.

The amplitude $h(x, t)$ must satisfy $h(x, t) = \bar{h}(t) + \frac{\sigma}{\lambda}\partial_x^{-2}q(x, t)$ where $\bar{h}(t)$ is undetermined by the evolution equation for q. To compute this time dependence consider $h(x, t)$ at the tip of the singularity; define

$$\bar{h}(t) = h(x_c, t). \tag{56}$$

Plugging the similarity solution into the equation for h gives

$$\bar{h}_t = -h_{xx}(x_c, t) - h_{xxxx}(x_c, t) + \sigma\lambda h_{xx}^2(x_c, t) + (1 - \lambda)h_x(x_c, t)^2$$

24

$$\sim \frac{\sigma \bar{C}}{\lambda(t_c - t)} + \mathcal{O}\left((t_c - t)^{-1/2}\right) \qquad \text{for} \qquad t_c - t \ll 1. \tag{57}$$

Hence

$$\bar{h}(t) \sim \bar{h}_0 - \frac{\sigma \bar{C}}{\lambda} \ln(t_c - t) + \mathcal{O}\left((t_c - t)^{1/2}\right), \tag{58}$$

where $\bar{h}_0$ is a constant of integration determined by the initial front location.

The similarity profile in the neighborhood of the singularity now provides the complete asymptotic behavior for the amplitude, h.

$$h(x,t) \sim \bar{h}(t) + \frac{\sigma}{\lambda} \int_0^\eta d\eta' \int_0^{\eta'} F(\eta'')d\eta''. \tag{59}$$

The double integral can be evaluated in the far-field of the singularity using the far-field expansion (55), and the fact that the area under the similarity profile vanishes (cf. 41),

$$h(x,t) \sim -\frac{4\bar{C}\sigma}{\lambda} \ln|x - x_c| + C_0 + \mathcal{O}\left((t_c - t)^{1/2}, \frac{t_c - t}{(x - x_c)^4}\right)$$
$$\text{for} \qquad (t_c - t)^{1/4} \ll |x - x_c| \ll 1, \tag{60}$$

where the constant C_0 is given by

$$C_0 = \bar{h}_0 + \frac{\sigma}{\lambda} \lim_{L \to \infty} \left\{ \int_0^L d\eta' \int_0^{\eta'} F(\eta'')d\eta'' + 4\bar{C} \ln L \right\}. \tag{61}$$

In summary, the amplitude $h(x,t)$ blows up like $\ln(t_c - t)$ at the point of singularity, x_c (cf. 58). The amplitude in the neighborhood of the singularity converges pointwise to a profile like $\ln|x - x_c|$ (cf. 60). In the next section we show numerical simulations of the PDE which show quite clearly that the blow up has precisely the behavior described here in the limit as $t \to t_c$.

6 Numerics

This section presents results from numerical simulations of the finite-time blow up in the 1D MKS:

$$h_t + h_{xx} + h_{xxxx} = (1 - \lambda)h_x^2 + \sigma\lambda h_{xx}^2. \tag{1D MKS}$$

The code used here is an adaptation of a code used in [11–13] to study singularity formation in degenerate fourth-order equations. The main features of

the code are that it is an implicit finite difference scheme with a self-similar dynamically adaptive mesh for extremely high resolution of the singularity and its scaling structure. The details of the numerical method are presented in the appendix.

We considered values of λ ranging from 0.1 to 1 and a number of different initial conditions. All of the finite-time singularities observed have identical self-similar profiles in a neighborhood of the singular point as $t \to t_c$. These singularities are observed for some initial conditions not included in the conditions in Theorem 3. Moreover, even when the initial data is not symmetric about the point of blow up, the singularity exhibits the same local *symmetric* similarity solution seen in the cases where the initial data is symmetric. These results suggest that this similarity solution is a *universal* behavior for blow up in these equations.

Since all the blow-up profiles are identical, we present data from just one case with $\lambda = 1$ on the periodic domain $[-4, 4]$. The initial condition (at $t = 0$) is

$$h(x) = 2 + 4\cos(\pi x/4) + 2\cos(\pi x/2) + \tfrac{1}{2}\cos(\pi x)$$

and blow up occurs at the origin at roughly $t_c = 0.02415$. The profile over five spatial periods is shown in Figure 5. The profile has a form reminiscent of direction solidification; a series of *fingers* are separated by deep *roots*. Figure 6 shows a close up of the singularity as it forms. At $x = 0$ the amplitude, $h(x, t)$, goes to infinity as the log of the time to singularity (cf. 58). Near the singularity $h(x, t)$ converges pointwise to to $-4\bar{C}\ln|x|$. As the singularity occurs in a finite time, the regions far from the singularity (i. e. the tip of the finger) remain in a transient phase and do not reflect a long time character of the system. Some profiles are convex, while some such as that shown in Figure 5 may have a second local maximum.

The second derivative, h_{xx}, which approximates the curvature in the near-planar limit, exhibits the self-similar behavior described in the previous section. Figure 7 shows h_{xx} near the singularity time. Although the figure resembles the similarity profile (Figure 4), note that length scales depicted on the axes in Figure 7 indicate that this is a small scale structure very close to the singularity time. We confirm that the evolution approaches the universal similarity profile by rescaling amplitudes and widths. Figure 8 depicts nineteen orders of magnitude of rescaled data with excellent agreement to the solution $F(\eta)$ of the similarity ODE. In accordance with the change of variables defined by (36) the similarity width is computed by multiplying x by $(h_{xx}(0)/F(0))^{1/2}$. The amplitude of h_{xx} is rescaled by dividing $h_{xx}(x)$ by $h_{xx}(0)/F(0)$. Since the solution shown here is symmetric, only values for $x \geq 0$ are shown.

In addition to confirming the similarity profile, we can directly verify that the blow up exhibits the time dependences (both power law exponents in $(t_c - t)$

and prefactors) predicted by the similarity solution. Figure 9 examines the time dependence of h_{xx}. Pictured are computed values of $\log_{10}|h_{xx}(0)|/F(0)$ vs. $\log_{10} d(|h_{xx}(0)|/F(0))/dt$. The solid line is a plot of the same data for the function $h_{xx}(0,t) = F(0)(t_c - t)^{-1/2}$ as predicted by the similarity solution (cf. 36). Note that there are *no free parameters* with which to fit this data.

The similarity solution predicts that the amplitude at the blow-up point, $h(0,t)$, should grow as the natural log of the time to singularity (cf. 58),

$$h(0,t) \sim \bar{h}_0 - \bar{C} \ln(t_c - t) + \mathcal{O}\left((t_c - t)^{1/2}\right) \tag{62}$$

Figure 10 shows this blow up for the solution to the 1D MKS. Since the previous figure demonstrates that $2\ln|h_{xx}(0)/F(0)| \sim -\ln(t_c - t)$ It is convenient to study the time dependence of the blow up in h by plotting it against $2\ln|h_{xx}(0)/F(0)|$. A linear fit to the data shows a slope of approximately 2.015, which agrees quite well with the slope of $\bar{C} \approx 2.010$ predicted by the similarity solution.

The numerical study presented here clearly demonstrates that the blow up observed conforms to the asymptotic theory for the first-type self-similar blow up presented in the previous section. Although we have presented a detailed study of only one evolution, our numerical studies suggest that this blow up study is generic over a large range of parameters and initial conditions.

7 Conclusions

This paper addresses the question of finite-time singularity formation in a modified Kuramoto-Sivashinsky equation,

$$h_t + \nabla^2 h + \nabla^4 h = (1 - \lambda)|\nabla h|^2 + \sigma\lambda \left(\nabla^2 h\right)^2 + \delta\lambda \left(h_{xx}h_{yy} - h_{xy}^2\right),$$

in one and two space dimensions on a periodic domain. Using the Fourier space method of Palais [50] coupled with the continuation Theorem 1 we prove that for certain ranges of parameter space and period length, there exist initial conditions that yield finite-time singularities in which a second derivative of the amplitude blows up. Focusing on the one-dimensional problem, we (1) elucidate a relationship between the parameters and initial conditions for which blow up occurs and the bifurcation structure of spatially periodic solutions to the equation and (2) propose a similarity solution for the asymptotic behavior of the blow up in h_{xx}.

The picture of the dynamics emerging is that in the Kuramoto-Sivashinsky limit (λ tending to zero) small and moderate amplitude initial conditions are attracted to some bounded attractor while sufficiently large initial conditions

lead to finite-time blow up. For λ greater than a critical value, associated with the transition from super to subcritical in the pitchfork bifurcation discussed in Section 4, arbitrarily small initial conditions can lead to finite-time singularities.

The similarity solution associated with this blow up has three important features: (a) it is symmetric about the blow-up point, (b) it is of 'first type' so that the similarity scalings may be determined from dimensional analysis, and (c) it has *no free parameters*. We confirm this behavior as an apparently universal route to blow up via numerical simulations of the 1D MKS. The numerics use a dynamically adaptive self-similar mesh for extremely high resolution of the blow-up profile.

This paper is to our knowledge the first to study the asymptotic behavior of blow up in equations of this type. The combination of the blow-up results with the bifurcation analysis here and in [53] is a first step in obtaining a complete understanding of the complex structure of solutions to this problem. We believe the similarity profile should also describe blow up in the related Sivashinsky equation which describes directional solidification [22,48,49,54] and the quadratic Cahn-Hilliard equation [23,49] which models clumping of microorganisms [19].

Some interesting open mathematical problems raised by the work here include a rigorous existence proof and a stability analysis of the similarity solution introduced here and the asymptotic behavior of blow in the 2D problem. Also the blow-up Theorems 3 and 4 prove a singularity in the second derivative of h however the similarity solution shows a logarithmic blow up in h itself. We conjecture that a sharper result is true.

The MKS equation describes the near-planar limit of an intrinsic equation of motion (1). We believe that the blow up in the MKS driven by the term $(\nabla^2 h)^2$ corresponds to an analogous blow up in (1) driven by the curvature squared term, K^2 [10]. The blow up in h (cf. Figure 5) corresponds to the formation of deep roots between 'fingers' of one phase. Presumably, when the width of a root becomes comparable to boundary layer thickness any local description of the dynamics breaks down and the full governing equations need to be considered. One possible treatment of this problem is to look for a local *defect* solution that matches to a solution to the amplitude equation far from the singularity. For example, in models of spiral defects in excitable media, the intrinsic equation of motion breaks down at the spiral core, where it can be matched to a local defect solution for the core [9]. A possible candidate for this local defect for the blow up considered here is the asymptotic model of a root between directional solidification fingers of Brattkus [14]. It is our hope that the study presented here will lead to a better understanding of the morphology of the formation of these structures.

Acknowledgements

Appendix: An Adaptive Mesh Scheme for Singularity Formation

Is this appendix we describe a self-similar adaptive mesh numerical method design to capture singularity formation; this code is an adaptation of a code used in [11–13] hence some of the language comes from these sources. The simulations use a conventional finite difference method. It is an implicit two-level scheme based on central differences.

The simulations are on a domain $[-l, l]$. The solutions are symmetric about $x = 0$ hence the equation is solved on the interval $[0, l]$, discretized by the N mesh points,

$$0 = x_1 < x_2 < \ldots < x_N = 1.$$

At each computational time level the arrays h_i and p_i, $i \in [1, ..., N]$, approximate $h(x, t)$ and $-h_{xx}(x, t)$, and v_j, $j \in [1, ..., N-1]$ approximates $h_{xxx}(x, t)$. The h_i and p_i values exist at the point x_i, while v_i is the computed third derivative at the center of the interval, $(x_i + x_{i+1})/2$. The following picture depicts these associations:

$$
\begin{array}{ccc}
x_i & v_i & x_{i+1} \\
\times & \rule{3cm}{0.4pt} & \times \\
h_i & & h_{i+1} \\
p_i & & p_{i+1}
\end{array}
$$

.

29
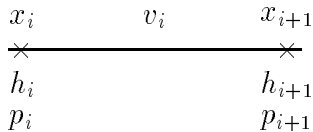
Using the notation:

$$\Delta x_{i+\frac{1}{2}} = x_{i+1} - x_i,$$

$$x_{i+\frac{1}{2}} = \tfrac{1}{2}(x_{i+1} + x_i),$$

$$\Delta x_i = x_{i+\frac{1}{2}} - x_{i-\frac{1}{2}},$$

$$h_{i+\frac{1}{2}} = \tfrac{1}{2}(h_{i+1} + h_i),$$

$$\partial h_i = (h_{i+1} - h_{i-1})/(x_{i+1} - x_{i-1}),$$

$$\partial h_{i+\frac{1}{2}} = \frac{h_{i+1} - h_i}{\Delta x_{i+\frac{1}{2}}},$$

$$\partial^2 h_i = \frac{\partial h_{i+\frac{1}{2}} - \partial h_{i-\frac{1}{2}}}{\Delta x_i},$$

The following describes the spatial discretization of the equation. Discretize the spatial operators by

$$(h_i)_t + \frac{v_i - v_{i-1}}{\Delta x_i} + p_i - (1-\lambda)(\partial h_i)^2 - \lambda p_i^2 = 0, \tag{63}$$

$$v_i + \partial p_{i+\frac{1}{2}} = 0, \tag{64}$$

$$p_i + \partial^2 h_i = 0. \tag{65}$$

The calculations presented here use symmetric initial data so that periodic boundary conditions can be imposed by reflection symmetry at the endpoints.

The time discretization of the above set of differential-algebraic relations uses a simple two-level scheme. In advancing from time t to time $t + dt$ a difference quotient replaces the time derivative term. The difference quotient involves the solution at the old time level (time t) and the as yet unknown solution at the new time level (time $t + dt$). The other terms in the equation use a weighted average of the solution at the two time levels; a typical weight is $\theta = 0.55$ on the advanced time level and $1 - \theta = 0.45$ on the old time level:

$$\frac{\partial h}{\partial t} = N(h)$$

would yield

$$\frac{1}{dt}\left(h_i(t + dt) - h_i(t)\right) = N\Big(0.55 h(\cdot, t + dt) + 0.45 h(\cdot, t)\Big).$$

At each time level, the code uses Newton's method to solve the set of nonlinear difference equations. By choosing an appropriate ordering of the $3N - 1$ equa-

tions (63–65), the Jacobi matrix has its nonzero entries close to the diagonal. For this reason, the use of Newton's method is not a prohibitive expense.

The length of the time steps adapts during the computation to control several aspects. If the result of the time step violates any of a list of constraints, it rejects the step and tries again with a smaller step size. To avoid using unnecessarily short time steps, if the the computation easily meet all the constraints for several steps, it increase the step size by about 20% on the next step. The first constraint comes from local time truncation. Another constraint rejects any step for which the maximum of $|h_{xx}|$ increases by more than 10%. Furthermore the correction on the first iteration of Newton's method must be a small fraction of the change over the step, where the initial guess at the change was the change over the previous step, corrected for any difference in dt's. Hence the method can solve the equations (63–65) in only one Newton iteration per time step, if desired.

The key part of the simulations needed to produce such high resolution of the singularity is a dynamically adaptive regridding scheme.

Self-similar adaptive mesh scheme

The method is straight forward and much simpler to implement than for instance the 'dynamic rescaling' proposed in [43,44] or the rescaling algorithm of Berger and Kohn [8].

In addition to ease of implementation this method is extremely efficient since it requires only $\mathcal{O}(|\log r|)$ mesh points to resolve a self-similar singularity to a width r. The computation described below took only a few minutes to run on a Sparc10 in double precision.

The method described here assumes a singularity at the origin. However, it can be generalized to a singularity at another point or a moving singularity. Initially start with a fixed mesh. The computation presented here uses an initial grid of $2^{10} = 1024$ uniform intervals. A second parameter is the number of grid points desired to resolve the singularity scale. In this calculation, this length scale is given by
$$\delta = (max|h_{xx}|)^{-1/2}$$
which can be thought of as the minimum length of the radius of curvature in the long wave limit. The calculation presented here uses 64 mesh points to resolve this length scale. When δ decreases to a width spanned by only 64 mesh points, the algorithm divides the first 64 intervals in half and defines this to be the new mesh. This division process is then repeated as the singularity forms, introducing 64 new mesh points with each regridding. This can be repeated *ad*

infinitum with only logarithmic dependence of the number of mesh points on the smallest scale resolved. Moreover, in this special case where the singularity occurs at $x = 0$, the fact that intervals are always halved exploits the binary arithmetic of of the computation and hence computes dx to infinite precision.

The simulation presented here goes through 55 levels of regridding, producing 3520 new points. Hence the smallest dx at the end of the simulation is $dx = 2^{-65}$. The values of h at each new mesh point are computed by linearly interpolating h_{xx} (computed from simple three point central differencing). The third derivative h_{xxx}, stored as a separate array throughout the calculation, is computed by linear interpolation.

References

[1] Robert A. Adams. *Sobolev spaces.* Academic Press, New York, 1975.

[2] Samuel M. Allen and John W. Cahn. A microscopic theory for antiphase boundary motion and its application to antiphase domain coarsening. *Acta Metallurgica*, 27:1085–1095, 1979.

[3] Dieter Armbruster, John Guckenheimer, and Philip Holmes. Kuramoto-Sivashinsky dynamics on the center-unstable manifold. *SIAM J. Appl. Math.*, 49:676–691, 1989.

[4] J. M. Ball. Remarks on blow-up and nonexistence theorems for nonlinear evolution equations. *Quart. J. Math. Oxford*, 28(2):473–486, 1977.

[5] G. I. Barenblatt. *Similarity, Self–Similiarity, and Intermediate Asymptotics.* Consultant's Bureau, Plenum Publishing Corp., New York, 1979.

[6] E. Ben-Jacob, Nigel Goldenfeld, J. S. Langer, and Gerd Schön. Boundary-layer model of pattern formation in solidification. *Phys. Rev. A*, 29:330–340, 1984.

[7] Carl M. Bender and Steven A. Orszag. *Advanced Mathematical Methods for Scientists and Engineers.* McGraw-Hill, 1978.

[8] Marsha Berger and Robert V. Kohn. A rescaling algorithm for the numerical calculation of blowing-up solutions. *Comm. Pur. Appl. Math*, 41:841–863, 1988.

[9] Andrew J. Bernoff. Spiral wave solutions for reaction-diffusion equations in a fast reaction/slow diffusion limit. *Physica D*, 53:125–150, 1991.

[10] Andrew J. Bernoff. Intrinsic equations of motion for reaction-diffusion equations. In preparation, 1994.

[11] A. L. Bertozzi. Loss and gain of regularity in a lubrication equation for thin viscous films. In J. I. Díaz, M. A. Herrero, A. Liñán, and J. L. Vázquez, editors, *Proceedings of the International Colloquium on Free Boundary Problems, Toledo, Spain, June 1993*, Pitman Research Notes in Mathematics. Pitman, 1994. to appear.

[12] Andrea L. Bertozzi. Symmetric singularity formation in lubrication-type equations for interface motion. submitted to *SIAM J. Applied Math.*

[13] Andrea L. Bertozzi, Michael P. Brenner, Todd F. Dupont, and Leo P. Kadanoff. Singularities and similarities in interface flow. In L. Sirovich, editor, *Trends and Perspectives in Applied Mathematics*, volume 100 of *Applied Mathematical Sciences*, pages 155–208. Springer–Verlag, New York, 1994.

[14] K. Brattkus. Capillary instabilities in deep cells during directional solidification. *J. Phys.*, 50:2999–3006, 1989.

[15] Richard C. Brower, David A. Kessler, Joel Koplik, and Herbert Levine. Geometrical approach to moving-interface dynamics. *Phys. Rev. Lett.*, 51:1111–1114, 1983.

[16] Richard C. Brower, David A. Kessler, Joel Koplik, and Herbert Levine. Geometrical models of interface evolution. *Phys. Rev. A*, 29:1335–1342, 1984.

[17] Chris Budd, Bill Dold, and Andrew Stuart. Blowup in a partial differential equation with conserved first integral. *SIAM J. Appl. Math.*, 53(3):718–742, June 1993.

[18] Yun-Gang Chen, Yoshikazu Giga, and Shun'ichi Goto. Uniqueness and existence of viscosity solutions to generalized mean curvature flow equations. *J. Diff Geom.*, 33:744–786, 1991.

[19] S. Childress and E. A. Spiegel. Pattern formation in a suspension of swimming microorganisms: nonlinear aspects. Unpublished manuscript.

[20] Pierre Collet, Jean-Pierre Eckmann, Henri Epstein, and Joachim Stubbe. Analyticity for the Kuramoto-Sivashinsky equation. *Physica D*, 67:321–326, 1993.

[21] Pierre Collet, Jean-Pierre Eckmann, Henri Epstein, and Joachim Stubbe. A global attracting set for the Kuramoto-Sivashinsky equation. *Commun. Math. Phys.*, 152:203–214, 1993.

[22] S. R. Coriell and G. B. McFadden. Morphological stability. In D. T. J. Hurle, editor, *Handbook of Crystal Growth*, volume 1, chapter 12, pages 785–857. Elsevier Science Publishers, 1993.

[23] Charles M. Elliott and Zheng Songmu. On the Cahn-Hilliard equation. *Arch. Rat. Mech. Anal.*, 96:339–357, 1986.

[24] L. C. Evans and J. Spruck. Motion of level sets by mean curvature. *J. Diff Geom.*, 33:635–681, 1991.

[25] Paul C. Fife. *Dynamics of Internal Layers and Diffusive Interfaces*. SIAM, 1988.

[26] M. L. Frankel. On the nonlinear evolution of a solid-liquid interface. *Phys. Lett. A*, 128:57–60, 1988.

[27] M. L. Frankel. On a free boundary problem associated with combustion and solidification. *Math. Modelling and Num. Anal.*, 23:283–291, 1989.

[28] M. L. Frankel and G. I. Sivashinsky. On the nonlinear thermal diffusive theory of curved flames. *J. Physique*, 48:25–28, 1987.

[29] M. L. Frankel and G. I. Sivashinsky. On the equation of a curved flame front. *Physica D*, 30:28–42, 1988.

[30] Y. Giga and R. V. Kohn. Asymptotically self-similar blow-up of semilinear heat equations. *Comm. Pur. Appl. Math.*, 38:297–319, 1985.

[31] Yoshikazu Giga and Robert V. Kohn. Characterizing blowup using similarity variables. *Indiana University Mathematics Journal*, 36(1):1–40, 1987.

[32] Jonathan Goodman. Stability of the Kuramoto-Sivanshinsky and related systems. *Comm. Pure Appl. Math.*, 47:293–306, 1994.

[33] Bruno Grossman, Hong Guo, and Martin Grant. Kinetic roughening of interfaces in driven systems. *Phys. Rev. A*, 43:1727–1741, 1991.

[34] John Guckenheimer and Philip Holmes. *Nonlinear Oscillations, Dynamical Systems, and Bifurcations of Vector Fields*. Springer-Verlag, 1983.

[35] Tal Hocherman and Philip Rosenau. On KS-type equations describing the evolution and rupture of a liquid interface. *Physica D*, 67:113–125, 1993.

[36] James M. Hyman, Amy Novick-Cohen, and Philip Rosenau. Modified asymptotic approach to modeling a dilute-binary-alloy solidification front. *Phys. Rev. B*, 37:7603–7608, 1988.

[37] Ju. S. Il'yashenko. Global analysis of the phase portrait for the Kuramoto-Sivashinsky equation. *Journal of Dynamics and Differential Equations*, 4(4):585–615, 1992.

[38] James P. Keener. A geometrical theory for spiral waves in excitable media. *SIAM J. Appl. Math*, 46:1039–1059, 1986.

[39] Ioannis G. Kevrikidis, Basil Nicolaenko, and James C. Scovel. Back in the saddle again: a computer-assisted study of the Kuramoto-Sivashinsky equation. *SIAM J. Appl. Math.*, 50:760–790, 1990.

[40] Sergiu Klainerman and Andrew Majda. Singular limits of quasilinear hyperbolic systems with large parameters and the incompressible limit of compressible fluids. *Comm. Pur. Appl. Math.*, 34:481–524, 1981.

[41] J. S. Langer. Instabilities and pattern formation in crystal growth. *Rev. Mod. Phys.*, 52:1–27, 1980.

[42] J. S. Langer. Lectures in the theory of pattern formation. In J. Souletie, J. Vannimeus, and R. Stora, editors, *Chance and Matter*, pages 629–711. North Holland, 1987.

[43] B. LeMesurier, G. Papanicolau, C. Sulem, and P-L. Sulem. The focusing singularity of the cubic Schrödinger equation. *Phys. Rev. A*, 34:1200–12010, 1986.

[44] B. LeMesurier, G. Papanicolau, C. Sulem, and P-L. Sulem. The focusing singularity of the nonlinear Schrödinger equation. In M. Crandall *et al*, editor, *Directions in Partial Differential Equations*, pages 159–201. Academic Press, New York, 1987.

[45] B. J. Matkowsky and G. I. Sivashinsky. An asymptotic derivation of two models in flame propagation theory associated with the constant density approximation. *SIAM J. Appl. Math.*, 37:686–699, 1979.

[46] B. Nicolaenko, B. Scheurer, and R. Temam. Some global dynamical properties of the Kuramoto-Sivashinsky equations: nonlinear stability and attractors. *Physica D*, 16:155–183, 1985.

[47] Basil Nicolaenko and Bruno Scheurer. Remarks on the Kuramoto-Sivashinsky equation. *Physica D*, 12:391–395, 1984.

[48] A. Novick-Cohen. Blow up and growth in the directional solidification of dilute binary alloys. Unpublished manuscript, 1987.

[49] A. Novick-Cohen. On Cahn-Hilliard type equations. *Nonlinear Analysis TMA*, 15(9):797–914, 1990.

[50] Bob Palais. Blowup for nonlinear equations using a comparison principle in Fourier space. *Commun. Pure Appl. Math.*, XLI:165–196, 1988.

[51] Pierre Pelcé. *Dynamics of Curved Fronts*. Perspectives in Physics, 1988.

[52] Jacob Rubinstein, Peter Sternberg, and Joseph B. Keller. Fast reaction, slow diffusion and curve shortening. *SIAM J. Appl. Math.*, 49:116–133, 1989.

[53] David C. Sarocka and Andrew J. Bernoff. An intrinsic equation of interfacial motion for the solidification of a pure hypercooled melt, 1994. submitted to Physica D.

[54] G. I. Sivashinsky. On cellular instability in the solidification of a dilute binary alloy. *Physica D*, 8:243–248, 1983.

[55] John J. Tyson and James P. Keener. Singular perturbation theory of traveling waves in excitable media (a review). *Physica D*, 30:327–361, 1988.

[56] A. Umantsev and S. H. Davis. Growth from a hypercooled melt near absolute stability. *Phys. Rev. A*, 45:7195–7201, 1992.

[57] J. J. Velazquez, V. A. Galaktionov, and M. A. Herrero. The space structure near a blow-up point for semilinear heat equations: A formal approach. *Comput. Maths. Math. Phys.*, 31(3):46–55, 1991.

[58] Hiroyasu Yamada and Kazuhiro Nozaki. Dynamics of wave fronts in excitable media. *Physica D*, 64:153–162, 1993.
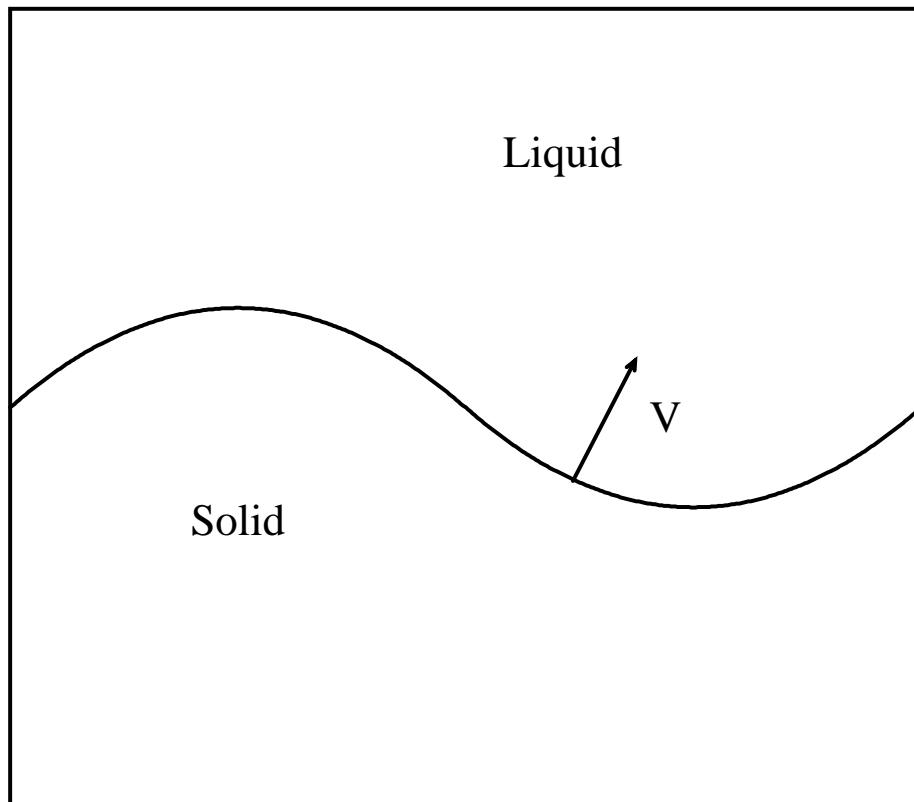
Intrinsic Equation of Interface Motion

Fig. 1. Intrinsic Equation of Interfacial Motion. The interface between two phases, here denoted solid and liquid (as in solidification) moves with normal velocity, V, at each point on the interface. The purely local dynamic coupling between points on the interface and the isotropy of the system suggest that only *local* geometric properties of the interface, such as the mean and Gaussian curvature, determine the velocity of the interface.

Periodic Solutions to 1D MKS

σ=1
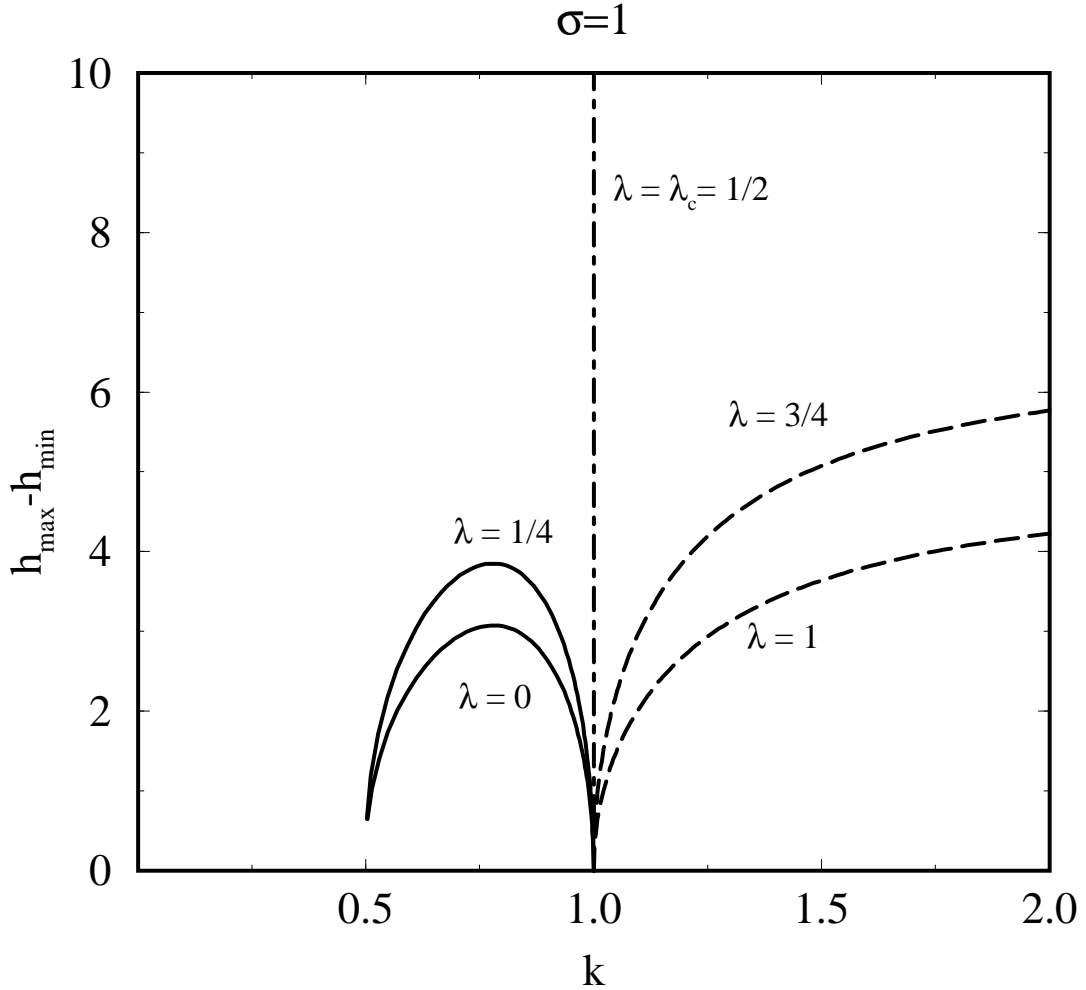
Fig. 2. Bifurcation of periodic solutions to the 1D MKS. We use a shooting method to compute the branch of periodic solutions bifurcating from $k = 1$. The amplitude between maximum and minimum height ($h_{max} - h_{min}$) is graphed as a function of wavenumber (k) for different values of λ. Note that for $\lambda < \lambda_c$ ($\lambda > \lambda_c$) the bifurcation is supercritical (subcritical) to a branch of solutions that are stable (unstable) at small amplitudes (to perturbations of the same periodicity); the stable (unstable) branch is denoted by a solid (dashed) line. At $\lambda = \lambda_c$ the bifurcation is vertical at leading order in the center manifold theory (dash-dot). (a) Bifurcations for $\sigma = 1$. Note that when $\lambda = \lambda_c = 1/2$ the bifurcation is perfectly vertical corresponding to a known exact (time dependent) solution. (b) Bifurcations for $\sigma = -1$. Here $\lambda_c = 1/3$; in this case the branch eventually veers off to larger k indicating instability.

Periodic Solutions to 1D MKS

σ=1
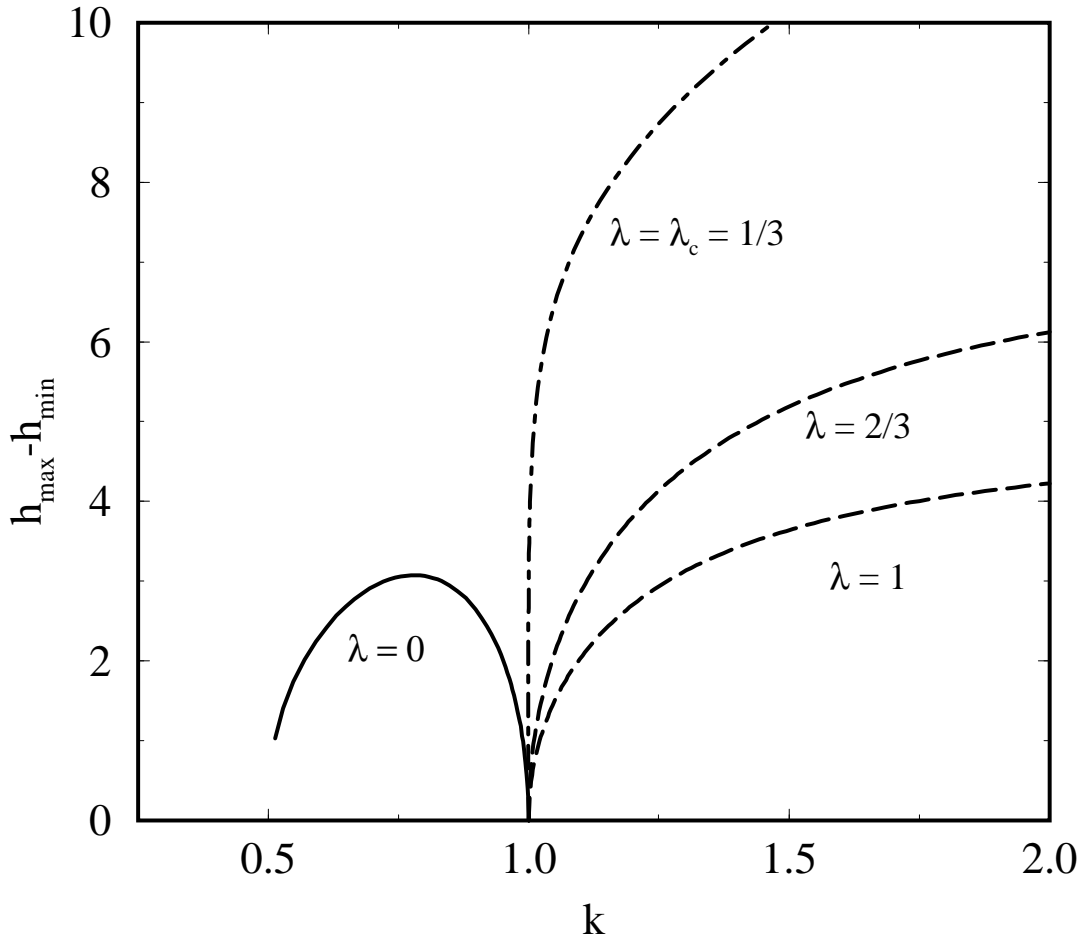
Fig. 2. (b) For caption see previous figure.

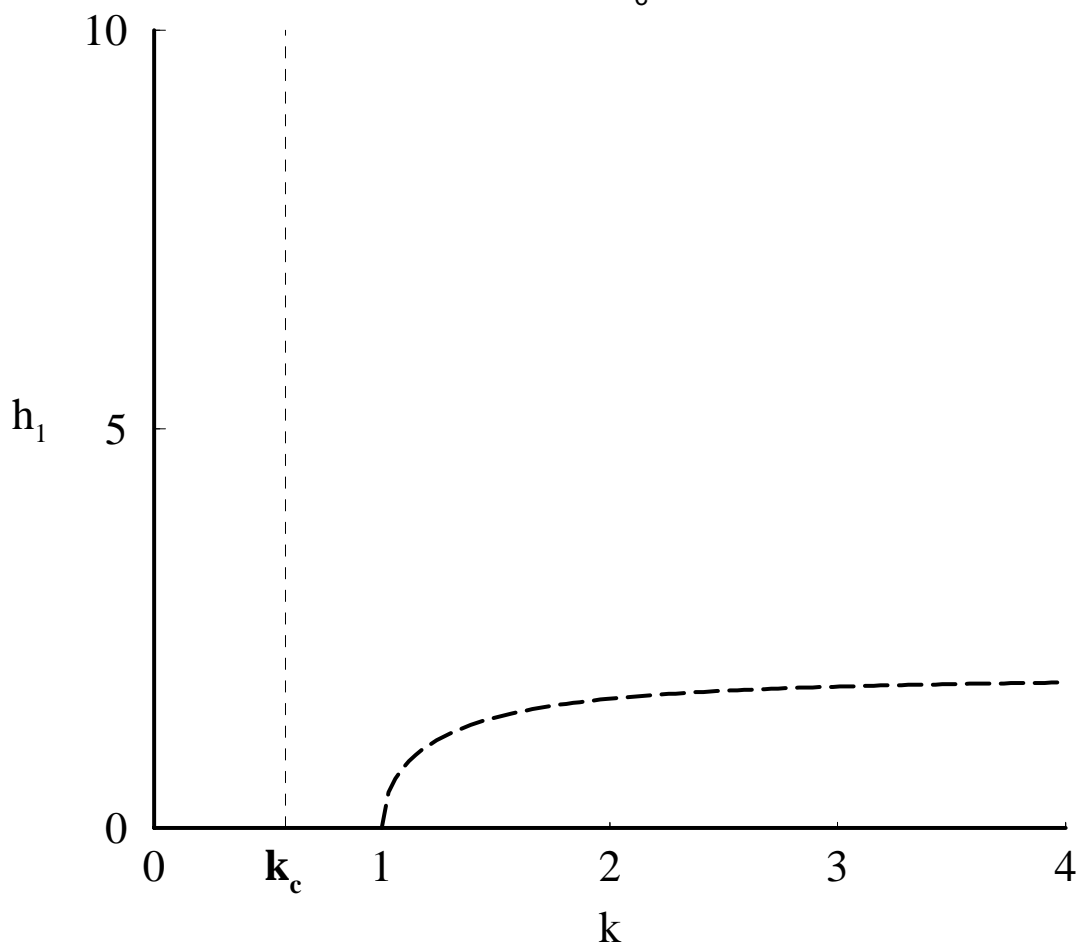## Steady states: 1-2 Subsytem

$$\lambda < \lambda_c$$
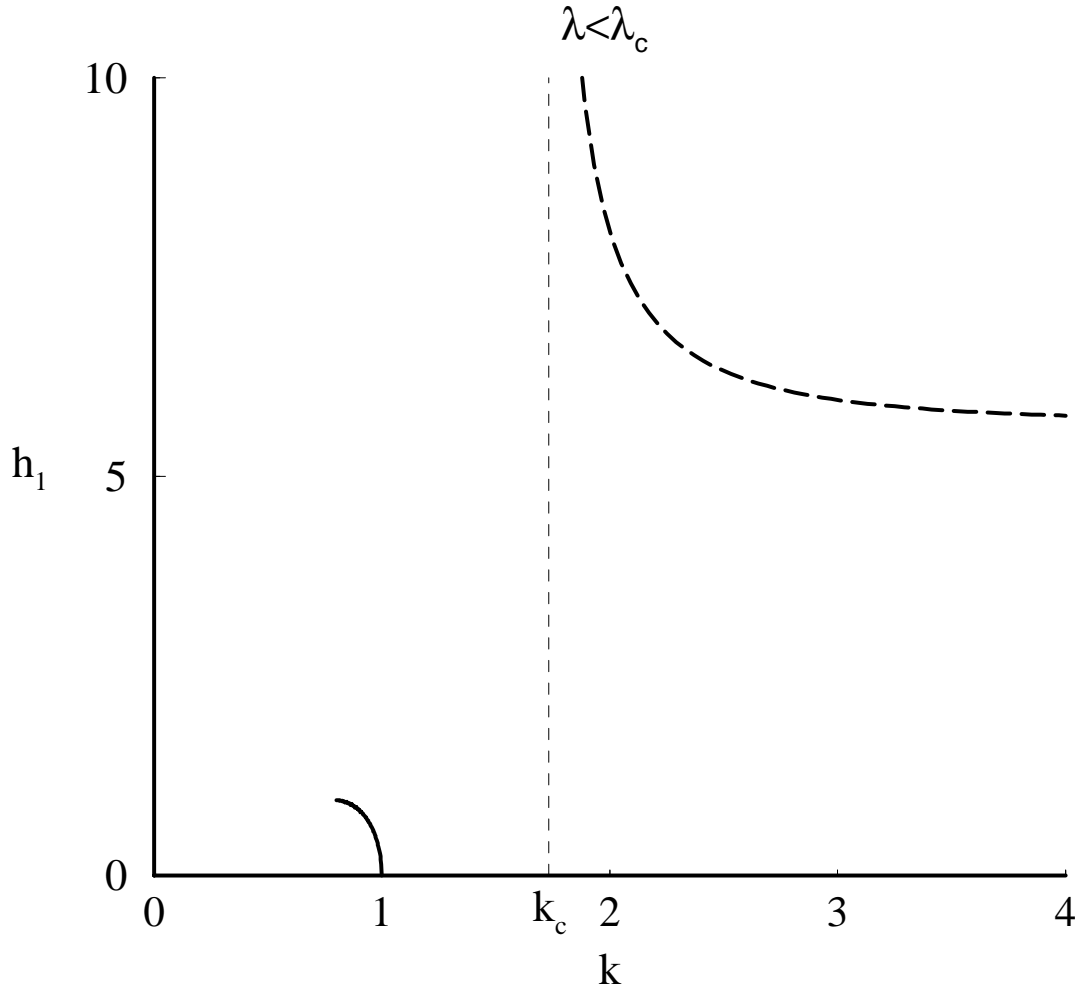
Fig. 3. Steady solutions to the 1-2 subsystem. (a) Supercritical case ($\lambda < \lambda_c$). Here the bifurcation to periodic solutions is supercritical and tangent to the bifurcation in the full problem. The system is cooperative for $k > k_c > 1$. At k_c a branch of unstable solutions bifurcates from infinity. Initial conditions that start "above" (in the sense of Theorem 3) this branch will tend to infinity, reflecting finite-time blow up in both the 1-2 subsystem and the full problem.

Steady States: 1-2 Subsystem
$\lambda > \lambda_c$

Fig. 3. Steady solutions to the 1-2 subsystem. (b) Subcritical case ($\lambda > \lambda_c$). Here the bifurcation to periodic solutions is subcritical and tangent to the bifurcation in the full problem. The system is cooperative for $k > k_c$, but in this case $k_c < 1$. For $k_c < k < 1$, a class of initial conditions of arbitrarily small amplitude leads to finite-time blow up in both the 1-2 subsystem and the full problem; for $k > 1$, initial conditions that start "above" (in the sense of Theorem 3) the unstable branch will also lead to finite-time blow up.

Similarity Profile for 1D MKS
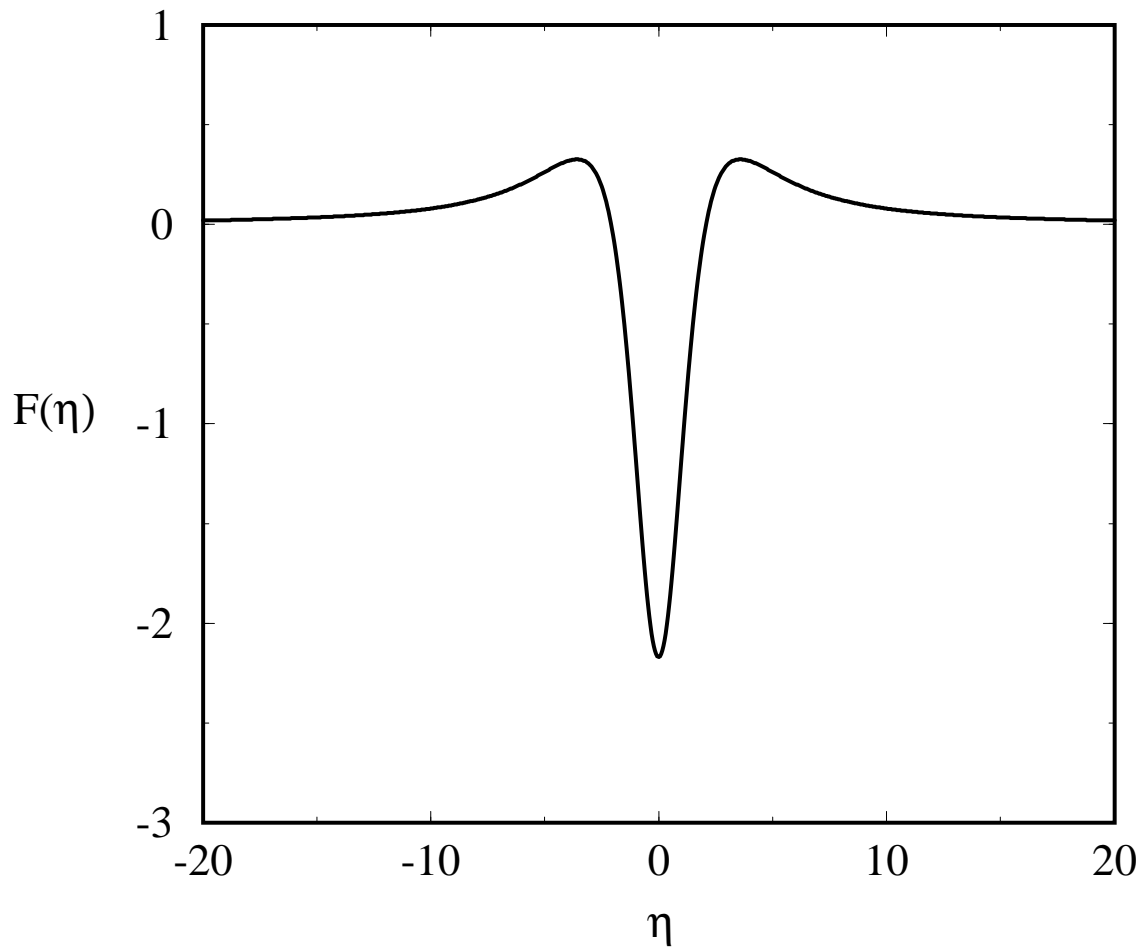
Fig. 4. Self-similar profile for blow up. A steady solution $F(\eta)$ to the ODE (45) describes the similarity profile for blow up in the second derivative h_{xx} of the amplitude. The solution is symmetric, obtains both positive and negative values, and tends to zero like $4\bar{C}/\eta^2$ for large $|\eta|$.
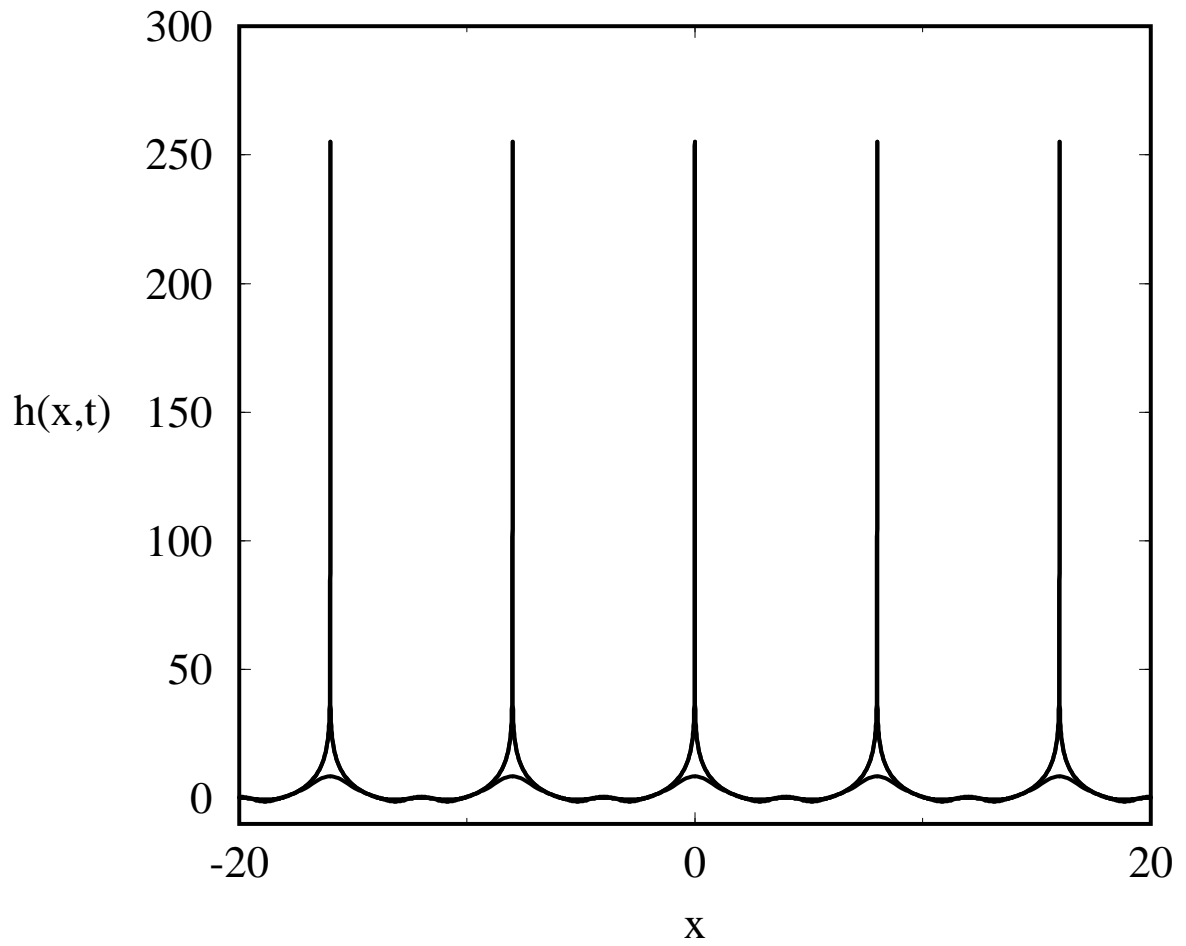
Blow Up in the 1D MKS

λ=1

Fig. 5. Blow up of a periodic initial condition ($\lambda = 1$). Typical profiles for a periodic initial condition as a function of time are shown. Note that the blow up occurs pointwise, reminiscent of the deep root formation between fingers often seen in directional solidification.

Close Up of Blow Up in h(x,t)

$\lambda=1$
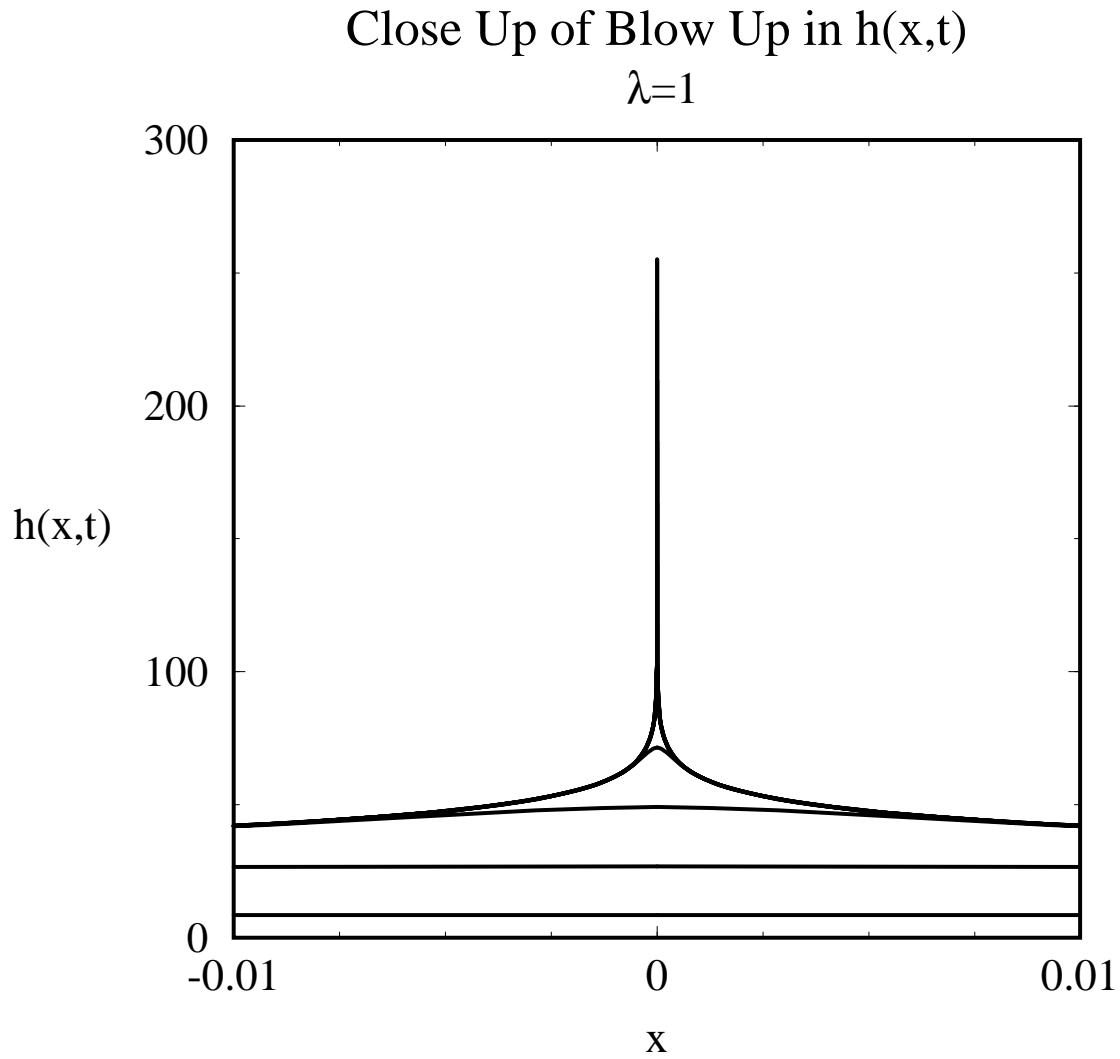
Fig. 6. Close up of the singularity formation ($\lambda = 1$). The height, $h(x,t)$ grows monotonically in time and develops a singularity at $x = 0$. The maximum height blows up as the log of $(t_c - t)$. Near the singularity the profile converges pointwise to $-4\bar{C}\ln|x|$.

Curvature (h$_{xx}$) Close to the Singularity Time
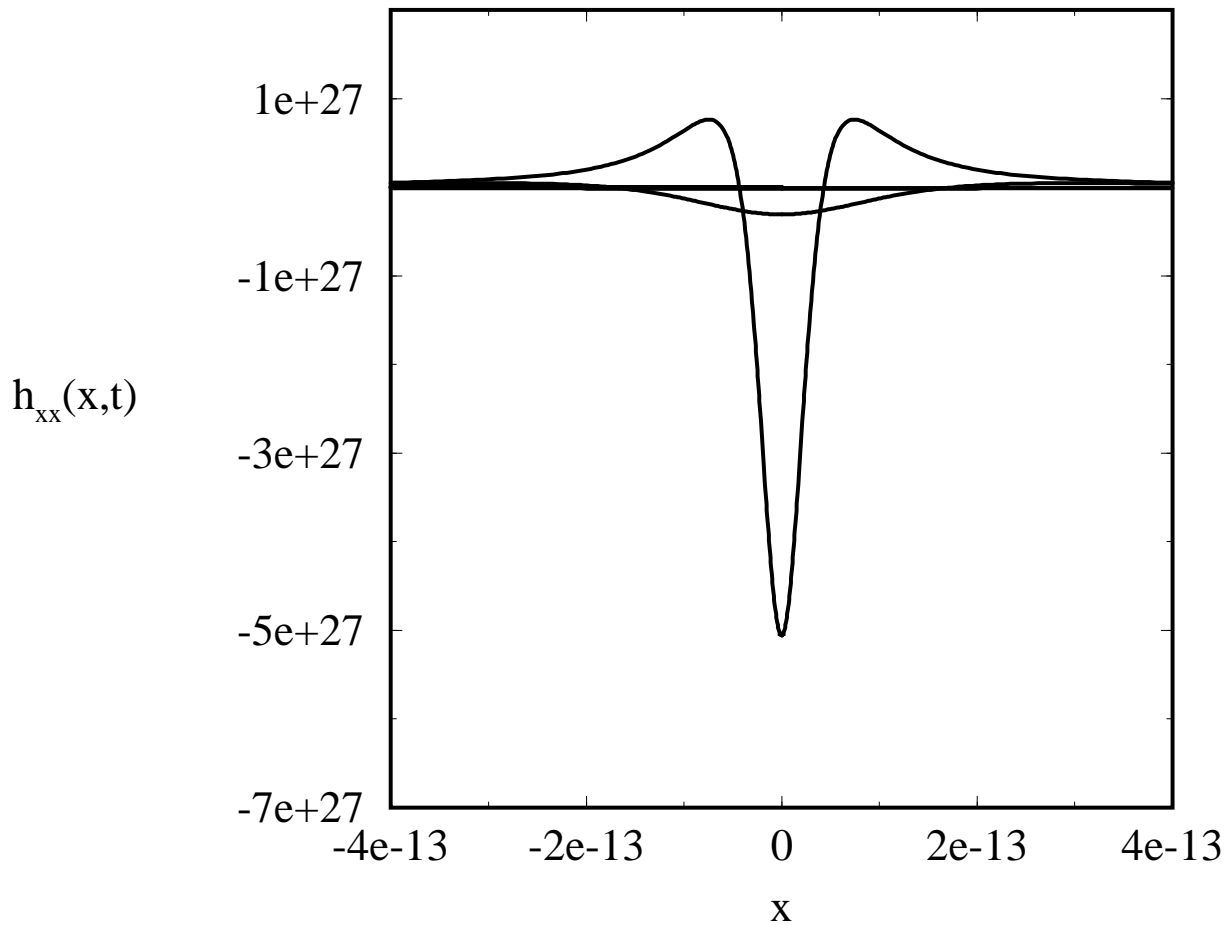## self-similar profile

Fig. 7. The curvature blow up close to the singularity time with $\lambda = 1$. Note the extreme magnitude of the scales. The profile clearly depicts the universal similarity shape (compare Figure 4).
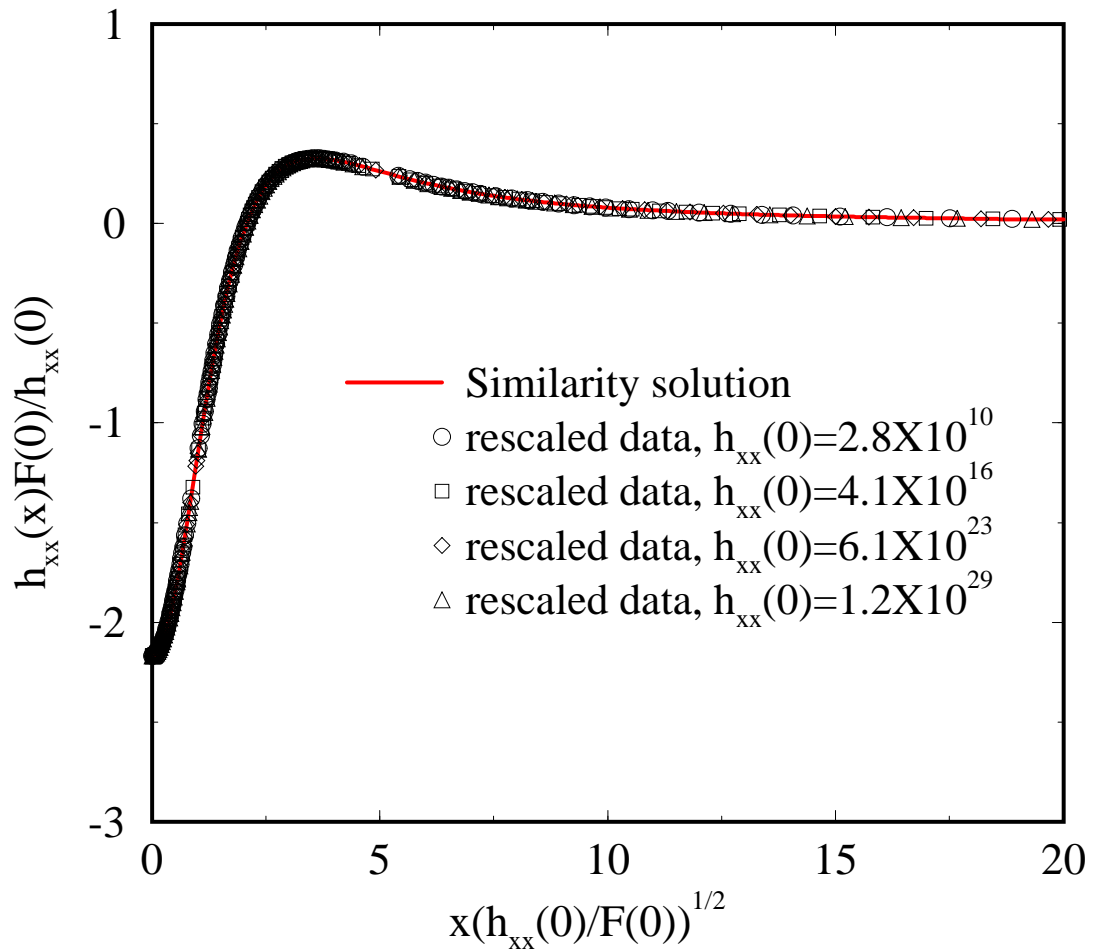
Fig. 8. Rescaled h_{xx} over nineteen orders of magnitude. The data is rescaled to similarity variables by multiplying x by $(h_{xx}(0)/F(0))^{1/2}$ and h_{xx} by $F(0)/h_{xx}(0)$, where $F(0)$ is fixed by the similarity solution. As the solution is symmetric only values for $x \geq 0$ are shown. The data shows excellent agreement of the blow up profile with the similarity solution (solid line graphed above) from Section 5.
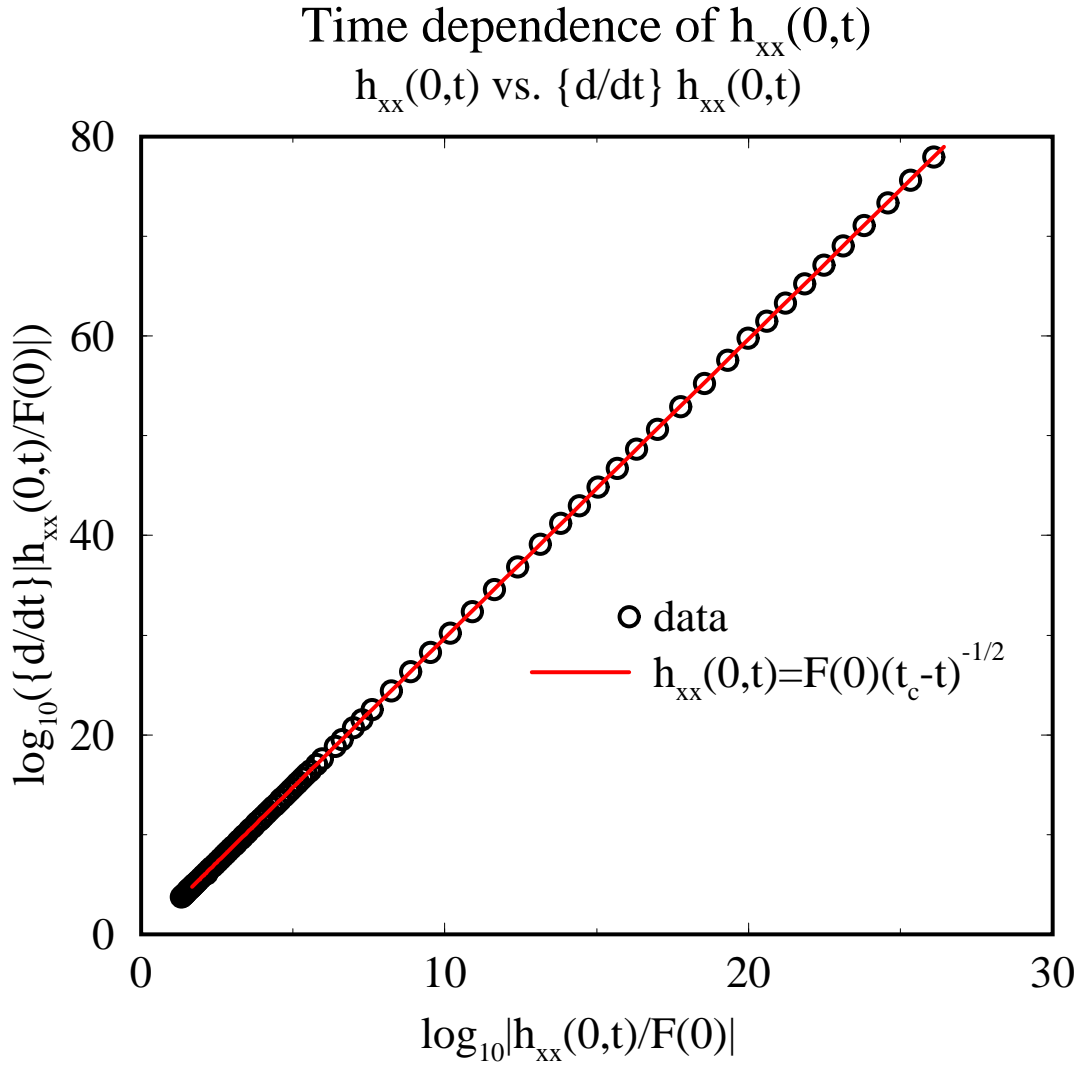
Fig. 9. Time dependence of $h_{xx}(0,t)$. Pictured are computed values of $log_{10}|h_{xx}(0,t)/F(0)|$ vs. $log_{10}d|h_{xx}(0,t)/F(0)|/dt$ compared with the predicted value from the similarity solution. Near blow up we expect $h_{xx}(0,t) \sim F(0)(t_c - t)^{-1/2}$, so there are *no free parameters* with which to fit the data to the similarity solution.
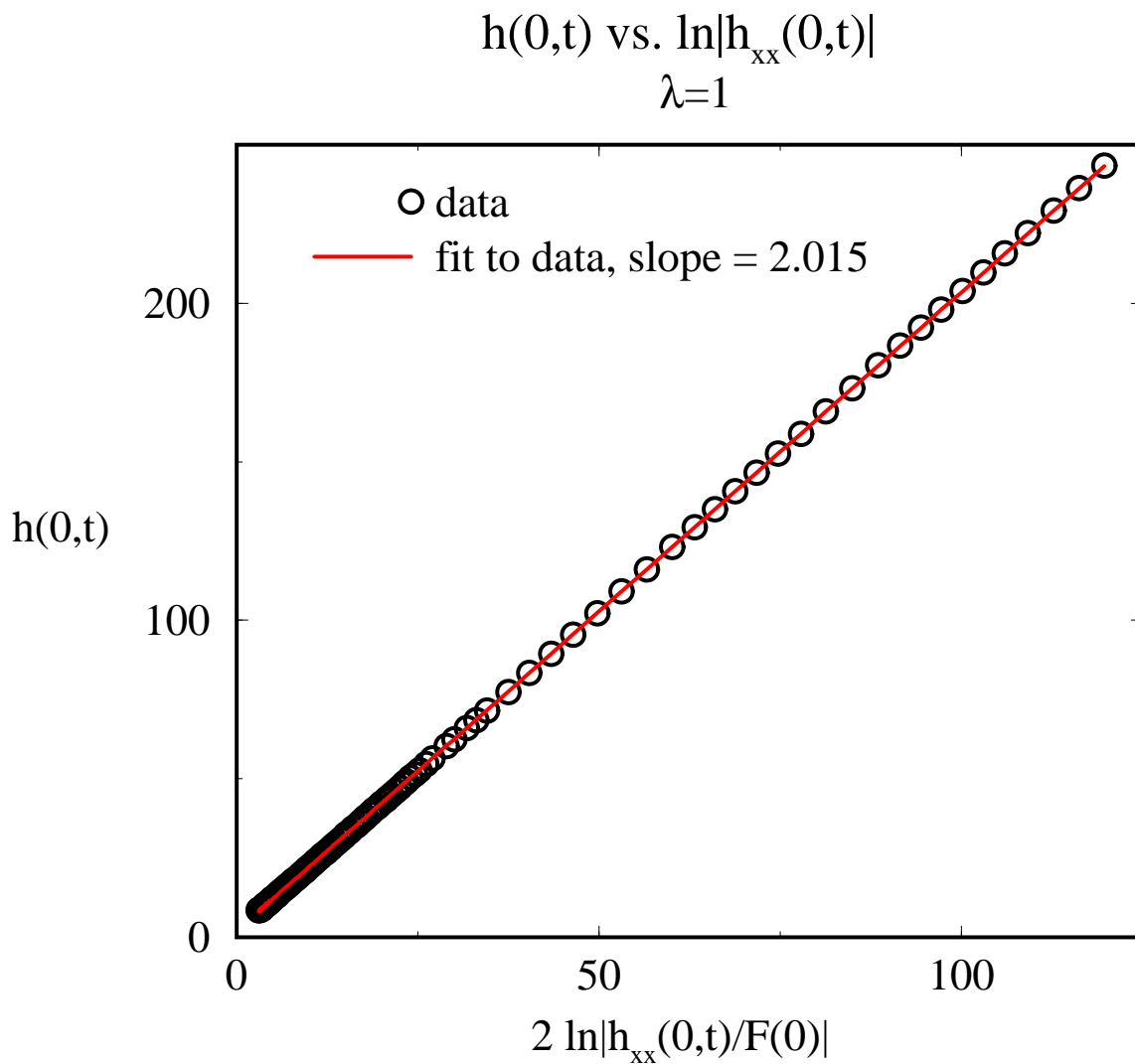
Fig. 10. Logarithmic blow up of height. Pictured $h(0,t)$ vs. $2\ln|h_{xx}(0)/F(0)|$. Recall that $|h_{xx}(0,t)/F(0)| \sim -\ln[t_c - t]$) (see e.g. Figure 9). By plotting $h(0,t)$ against $2\ln|h_{xx}(0)/F(0)|$ we show that $h(0,t)$ blows up as the natural log of $(t_c - t)$. The slope of 2.015 from a linear regression of the data agrees quite well with the expected value $\bar{C} \approx 2.010$ from the similarity solution.